Clim. Past, 6, 531–552, 2010
www.clim-past.net/6/531/2010/
doi:10.5194/cp-6-531-2010

Climate of the Past

Variations in mid-latitude North Atlantic surface water properties during the mid-Brunhes (MIS 9–14) and their implications for the thermohaline circulation

A. H. L. Voelker[1,2], T. Rodrigues[1,2], K. Billups[3], D. Oppo[4], J. McManus[4,*], R. Stein[5], J. Hefter[5], and J. O. Grimalt[6]

[1]Unidade Geologia Marinha, Laboratorio Nacional de Energia e Geologia (LNEG; ex-INETI), Estrada da Portela, Zambujal, 2610-143 Amadora, Portugal
[2]CIMAR Associate Laboratory, Rua dos Bragas 289, 4050-123 Porto, Portugal
[3]College of Earth, Ocean, and Environment, University of Delaware, 700 Pilottown Road, Lewes, DE 19958, USA
[4]Geology and Geophysics, Woods Hole Oceanographic Institution, Woods Hole, MA 02543, USA
[5]Alfred-Wegener-Institute for Polar and Marine Research, Columbusstrasse, 27568 Bremerhaven, Germany
[6]Department of Environmental Chemistry, Institute of Environmental Assessment and Water Research (IDÆA–CSIC), Jordi Girona 18, 08034-Barcelona, Spain
[*]now at: Department of Earth and Environmental Science, Columbia University, Lamont-Doherty Earth Observatory, 61 Route 9W, Palisades, NY 10964-8000, USA

Received: 16 May 2009 – Published in Clim. Past Discuss.: 3 June 2009
Revised: 22 July 2010 – Accepted: 11 August 2010 – Published: 27 August 2010

Abstract. Stable isotope and ice-rafted debris records from three core sites in the mid-latitude North Atlantic (IODP Site U1313, MD01-2446, MD03-2699) are combined with records of ODP Sites 1056/1058 and 980 to reconstruct hydrographic conditions during the middle Pleistocene spanning Marine Isotope Stages (MIS) 9–14 (300–540 ka). Core MD03-2699 is the first high-resolution mid-Brunhes record from the North Atlantic's eastern boundary upwelling system covering the complete MIS 11c interval and MIS 13. The array of sites reflect western and eastern basin boundary current as well as north to south transect sampling of subpolar and transitional water masses and allow the reconstruction of transport pathways in the upper limb of the North Atlantic's circulation. Hydrographic conditions in the surface and deep ocean during peak interglacial MIS 9 and 11 were similar among all the sites with relative stable conditions and confirm prolonged warmth during MIS 11c also for the mid-latitudes. Sea surface temperature (SST) reconstructions further reveal that in the mid-latitude North Atlantic MIS 11c is associated with two plateaus, the younger one of which is slightly warmer. Enhanced subsurface northward heat transport in the eastern boundary current system, especially during early MIS 11c, is denoted by the presence of tropical planktic foraminifer species and raises the question how strongly it impacted the Portuguese upwelling system. Deep water ventilation at the onset of MIS 11c significantly preceded surface water ventilation. Although MIS 13 was generally colder and more variable than the younger interglacials the surface water circulation scheme was the same. The greatest differences between the sites existed during the glacial inceptions and glacials. Then a north – south trending hydrographic front separated the nearshore and offshore waters off Portugal. While offshore waters originated from the North Atlantic Current as indicated by the similarities between the records of IODP Site U1313, ODP Site 980 and MD01-2446, nearshore waters as recorded in core MD03-2699 derived from the Azores Current and thus the subtropical gyre. Except for MIS 12, Azores Current influence seems to be related to eastern boundary system dynamics and not to changes in the Atlantic overturning circulation.

Correspondence to: A. Voelker
(antje.voelker@lneg.pt)

Published by Copernicus Publications on behalf of the European Geosciences Union.

1 Introduction

The Brunhes polarity chron encompasses the last 780 ka (kiloannum = thousand year) and its middle section is often considered as a particularly warm period during the last 1000 ka, when warm surface waters penetrated polewards and sea levels were generally higher than at Present (Droxler et al., 2003). MIS 11 and 9 are part of this warm interval. Interglacial MIS 11c was the first interglacial period after the mid-Pleistocene transition with atmospheric greenhouse gas concentrations and temperatures over Antarctica (Petit et al., 1999; Siegenthaler et al., 2005; Spahni et al., 2005; Jouzel et al., 2007) at levels similar to those during subsequent interglacials including the Holocene. Based on temperature related proxy records from the oceans (Hodell et al., 2000; Lea et al., 2003; McManus et al., 2003; de Abreu et al., 2005; Helmke et al., 2008) and from Antarctica (Petit et al., 1999; Jouzel et al., 2007) it was an unusually long lasting interglacial and northern heat piracy, i.e. the enhanced advection of warm waters from the South into the North Atlantic, was at its maximum (Berger and Wefer, 2003). The enhanced and prolonged northward heat flux led to relative mild conditions on Greenland and the development of a boreal coniferous forest indicating a major reduction of the ice shield (de Vernal and Hillaire-Marcel, 2008). The early temperature rise during the high amplitude transition from glacial MIS 12 to MIS 11c leads to two possible definitions for the duration of the interglacial period within MIS 11. Based on the interval of maximum warmth in marine records, the interglacial period lasted at minimum from to 420 to 396 ka (McManus et al., 2003; Helmke et al., 2008). The definition of an interglacial as the period of ice volume minimum/sea-level highstand (Shackleton, 1969), however, shortens this interval to 409 to 396 ka (based on the LR04 chronology; Lisiecki and Raymo, 2005). This shorter period is also the interval, when full interglacial conditions occurred in the Nordic Seas (Bauch et al., 2000). Because of the similarity in the eccentricity signal (Loutre and Berger, 2003), MIS 11c is the interglacial often used as equivalent to the Holocene. In the subpolar North Atlantic at ODP Site 980 MIS 11c is recorded as a long, stable interval with relatively small SST variations (Oppo et al., 1998; McManus et al., 2003), while the later phase of MIS 11, contemporary with the built-up of continental ice sheets during the inception of glacial MIS 10, is marked by millennial-scale variability linked to ice-rafting events and southward incursions of arctic surface waters (Oppo et al., 1998; McManus et al., 1999). On the western boundary of the subtropical gyre at ODP Site 1056, on the other hand, peak interglacial conditions were more variable in the surface water as evidenced by short-term incursions of colder surface waters, while thermocline conditions were relative stable and comparable to the Holocene (Chaisson et al., 2002; Billups et al., 2004). During the transition to MIS 10 the Gulf Stream waters at ODP Site 1056 experienced higher temperature variability linked to cooling episodes in the surface and thermocline waters (Chaisson et al., 2002; Billups et al., 2004), episodes that are contemporary with those recorded at ODP Site 980.

The interglacial after MIS 11c was MIS 9e – following (Tzedakis et al., 1997) MIS 9 is divided into five substages. MIS 9e is a better analog for the Holocene than MIS 11c if tilt and insolation are emphasized for the comparison (Ruddiman, 2006). During MIS 9e ice volume minimum and temperature maximum coincided (e.g., McManus et al., 1999; Martrat et al., 2007) with the sea-level highstand being dated approximately to 334 to 306 ka (Stirling et al., 2001). In the Antarctic ice core records, MIS 9e is marked by an early maximum in temperature (Petit et al., 1999; Watanabe et al., 2003; Jouzel et al., 2007) and greenhouse gas concentrations (Petit et al., 1999; Loulergue et al., 2008), when values even exceeded pre-industrial Holocene levels. Such an overshooting is, however, not seen in high-resolution marine or terrestrial records from the Northern Hemisphere (McManus et al., 1999; Prokopenko et al., 2002; Tzedakis et al., 2004; Martrat et al., 2007; Desprat et al., 2008; Tzedakis et al., 2009).

As mentioned above, MIS 11c marked a transition in interglacial conditions, the so called Mid-Brunhes Event (Jansen et al., 1986; Wang et al., 2003; Barker et al., 2006; Yin and Berger, 2010). Mid-Pleistocene interglacials prior to MIS 11c were colder in Antarctica (EPICA Members, 2004) and had lower carbon dioxide concentrations (Siegenthaler et al., 2005; Lüthi et al., 2008). The LR04 benthic stack (Lisiecki and Raymo, 2005) clearly reveals that ice volume was larger during MIS 13 than during MIS 11 or 9. In terrestrial records from Tenaghi Philippon (Tzedakis et al., 2006), Lake Baikal (Prokopenko et al., 2002) or the Chinese Loess Plateau (Guo et al., 2000), on the other hand, MIS 13 does not differ greatly from some of the subsequent interglacials, especially MIS 11. Besides these differences in climatic responses on land and in the ocean, MIS 13 is unique in the timing of full interglacial conditions. Maximum warmth and ice volume minimum of all the other interglacials during the last 700 ka occurred during the first substage after the Termination, i.e. after the transition from a glacial maximum to the interglacial sea-level highstand. During MIS 13, however, the interval of ice volume minimum (Lisiecki and Raymo, 2005) and maximum warmth in the EDC ice core record (Jouzel et al., 2007) coincided not with the first, but with the third substage, MIS 13a. Thus we regard MIS 13a as the full interglacial interval within MIS 13, even if atmospheric carbon dioxide concentrations were at a similar level during both warm substages, MIS 13c and 13a (Siegenthaler et al., 2005), and nitrous dioxide peaked during MIS 13c (Spahni et al., 2005).

One of the reasons why MIS 13 is so different, might be that its preceding glacial, MIS 14, was so weak with sea level lowering only about as half as during MIS 16, 12 or 10. Consequently, also the amplitude of Termination VI was much lower than during Terminations V or IV. MIS 12, on the other hand, was one of the most extreme glacials during the last 1000 ka, when sea level was probably lower than during the

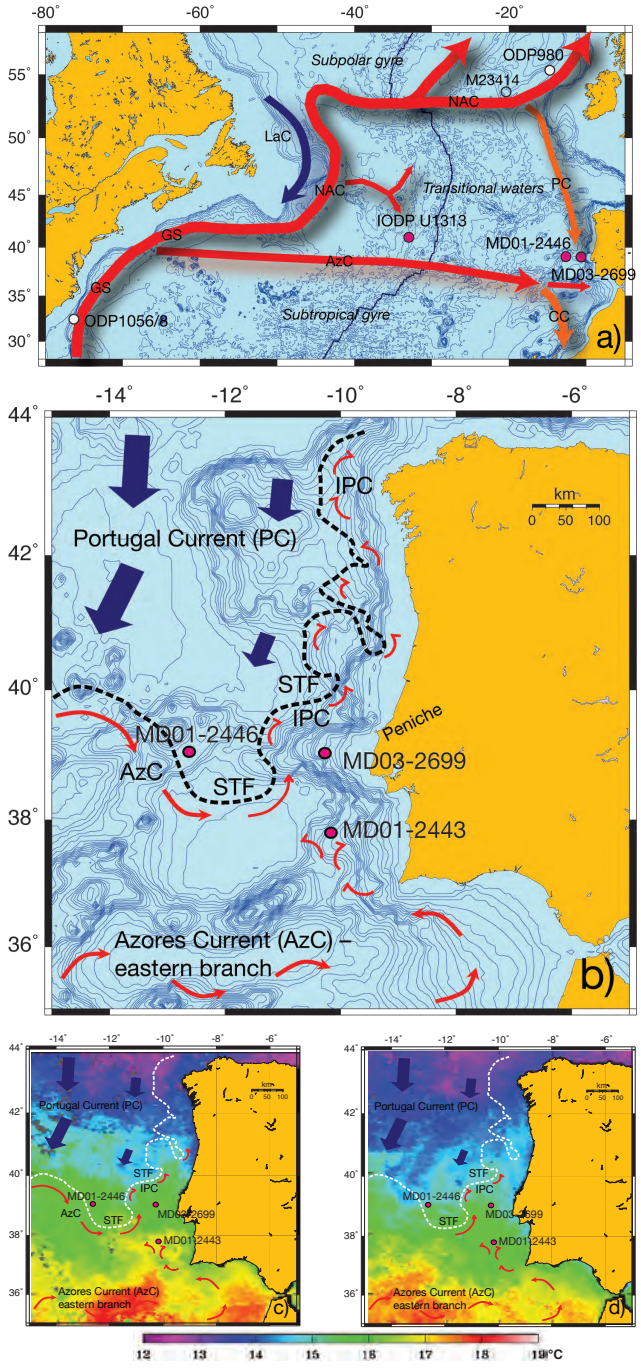

Fig. 1. **(a)** Core locations and major surface water currents in the North Atlantic (Fratantoni, 2001): GS = Gulf Stream; NAC = North Atlantic Current; AzC = Azores Current; CC = Canary Current; PC = Portugal Current; LaC = Labrador Current. **(b)** Winter circulation scheme off Portugal after Peliz et al. (2005) with IPC = Iberian Poleward Current and STF = Subtropical front. **(c)** and **(d)** Satellite derived sea surface temperatures (AVHRR Pathfinder Version 5; http://poet.jpl.nasa.gov) for January 2002 (c) and February 2007 (d) (monthly means) for the Iberian margin – both cases with the IPC present – indicate that temperature gradients between the three sites can vary between 0 and 1.5 °C. Currents and fronts, if depicted, as in (b).

last glacial maximum (MIS 2) (Lisiecki and Raymo, 2005). Sea level during MIS 10 was similar to MIS 2, even though MIS 10 lasted only half as long as MIS 12. In regard to dust flux in Antarctica MIS 14 is also the weakest and MIS 12 the strongest glacial (Lambert et al., 2008). This pronounced difference between the mid-Brunhes glacials is, however, not evident in the EDC temperature and greenhouse gas records (Jouzel et al., 2007; Loulergue et al., 2008; Lüthi et al., 2008).

One of the most prominent features of the last glacial inception is the periodic occurrence of major ice-rafting events, the so called Heinrich events (e.g., Hemming, 2004). During the Brunhes chron Heinrich-type ice-rafting events were first observed at the end of MIS 16 (Hodell et al., 2008) and then more regularly within MIS 12 and 10 (McManus et al., 1999; Hodell et al., 2008; Ji et al., 2009). McManus et al. (1999) showed that the onset of millennial-scale climate variability, including ice-rafting events, is linked to a threshold value of 3.5‰ in benthic δ^{18}O. As soon as this ice volume threshold was passed the Atlantic meridional overturning circulation (AMOC) became less stable resulting in oscillations between weaker and stronger AMOC modes. Most of the existing evidence for millennial-scale AMOC variability during the mid-Brunhes and its impacts on surface and deep waters is linked to the inception of MIS 10 (Poli et al., 2000; Billups et al., 2004; de Abreu et al., 2005; Hall and Becker, 2007; Martrat et al., 2007; Dickson et al., 2008; Stein et al., 2009). Only records from ODP Sites 980 and 1058 cover the older glacials with sufficient resolution (McManus et al., 1999; Flower et al., 2000; Billups et al., 2006; Weirauch et al., 2008) and here we present the previously unpublished planktic δ^{13}C records for these sites.

Results of this study increase the geographical coverage of proxy records to more fully characterize North Atlantic paleoceanography during the mid-Brunhes. With these proxy records we can assess similarities and differences in hydrographic conditions in the mid-latitude North Atlantic. This region encompasses the southern edge of the North Atlantic ice-rafted debris (IRD) belt (Ruddiman, 1977; Hemming, 2004) where large SST gradients occurred during glacials (Calvo et al., 2001; Pflaumann et al., 2003) and stadials (Chapman and Maslin, 1999; Oppo et al., 2001). The two new records off Portugal, MD01-2446 and MD03-2699, allow for the first time the reconstruction and evaluation of the full transition from glacial MIS 12 to interglacial MIS 11c in this eastern boundary upwelling system. By combining the planktic foraminifer stable isotope records from three new sites in the mid-latitude North Atlantic Ocean with those from ODP Sites 980 and 1056/1058 we aim (1) to map hydrographic conditions within the major surface currents (Fig. 1) and thus to identify potential latitudinal or longitudinal gradients in the North Atlantic during the interval spanning from MIS 9c to 14 (300–540 ka); (2) to trace the potential sources of the subsurface waters, which are essential in providing nutrients to sustain plankton productivity,

Table 1. Locations of core sites and their respective hydrographic and productivity regimes.

Site	Latitude	Longitude	Water depth	Surface water sources	Productivity regime
ODP Site 980	55°29.09′ N	14°42.13′ W	2168 m	Rockall Trough branch of North Atlantic Current	Subpolar regime
IODP Site U1313	41°00.07′ N	32°57.40′ W	3412 m	North Atlantic Current derived waters	Transitional zone between subpolar and mid-latitude regimes
MD01-2446	39°03.35′ N	12°37.44′ W	3570 m	Portugal Current	Mid-latitude regime
MD03-2669	39°02.20′ N	10°39.63′ W	1895 m	Upwelling and Iberian Poleward Current	Seasonal upwelling
MD01-2443	37°52.89′ N	10°10.57′ W	2941 m	Upwelling and Iberian Poleward Current	Seasonal upwelling
ODP Site 1056	32°29.10′ N	76°19.80′ W	2167 m	Gulf Stream	Subtropical regime
ODP Site 1058	31°41.40′ N	75°25.80′ W	2985 m		

and their changes on glacial and interglacial timescales; and (3) to address the question, how stable or variable hydrographic conditions were in the mid-latitude North Atlantic during MIS 11 and how they differed from those during its neighboring interglacials, MIS 13 and 9. Our interpretation is supported by IRD records for the three new sites and for alkenone-based SST data for MIS 11 from two of those sites. The first two objectives allow us to reconstruct circulation schemes for the upper limb of the North Atlantic's circulation and to identify pathways of heat, salt and nutrient transport in the surface to shallow subsurface ocean. Knowledge on those is essential in verifying how well coupled ocean-atmosphere models for the respective interglacials represent the AMOC.

2 Core sites and modern hydrographic setting

The three new core sites are IODP Site U1313, MD01-2446 and MD03-2699 (Table 1; Fig. 1). IODP Site U1313, which re-occupies the position of DSDP Site 607, was drilled in 2005 with *R/V Joides Resolution* during International Ocean Drilling Program (IODP) Expedition 306 (Channell et al., 2006). Calypso piston cores MD01-2446 and MD03-2699 were retrieved with *R/V Marion Dufresne* during the Geosciences cruise in 2001 and the PICABIA cruise in 2003, respectively. For tracing central/mode water masses within in the North Atlantic we combine the new records with those of ODP Site 980 in the subpolar North Atlantic and of ODP Sites 1056 and 1058 from the western subtropical gyre (Table 1, Fig. 1a).

Surface waters at all sites are derived in one form or another from the Gulf Stream and the North Atlantic Current (NAC). ODP Sites 1056 and 1058 are located directly below the Gulf Stream, while ODP Site 980 is influenced by the Rockall Trough branch of the NAC (Fratantoni, 2001; Brambilla and Talley, 2008). Even though IODP Site U1313 is located south of the core NAC pathway, drifter data shows that surface waters in this area are derived from the NAC, partly through recirculation off the Grand Banks (Fratantoni, 2001; Reverdin et al., 2003).

Gulf Stream/NAC derived surface waters off the western Iberian Peninsula are transported by two currents, the Portugal Current and the Azores Current (Fig. 1a–d). The Portugal Current (PC) is the NAC recirculation branch within the northeastern North Atlantic and is centered west of 10° W off Portugal (Fig. 1b; Peliz et al., 2005). The PC advects freshly ventilated surface and subsurface waters slowly southward. The subsurface component of the PC is subpolar Eastern North Atlantic Central Water (ENACW) that is formed by winter cooling in the eastern North Atlantic (McCartney and Talley, 1982), including along the NAC's Rockall Trough branch (Brambilla and Talley, 2008). The Azores Current (AzC) diverges from the Gulf Stream and moves in large meanders between 35 and 37° N across the North Atlantic. Its northern boundary forms the subtropical Azores front. In the eastern basin the AzC splits into several branches, one of which is the Canary Current, its major recirculation, and another, the eastern branch, enters into the Gulf of Cadiz (Fig. 1). During winter, waters from this eastern branch recirculate northward as the Iberian Poleward Current (IPC; Fig. 1b–d; Peliz et al., 2005), thereby bending the subtropical front northward along the western Iberian margin. Similar to the PC, the IPC includes a subsurface component: ENACW of subtropical origin. Subtropical ENACW is formed by strong evaporation and winter cooling along the Azores front (Rios et al., 1992) and is less ventilated, warmer and saltier than its subpolar counterpart (van Aken, 2001). During spring and summer (mainly May to September), on the other hand, the upwelling filaments that form off Peniche and Cape Roca can reach as far offshore as site MD03-2699, so that either upwelled waters or the seasonal, nearshore branch of the PC (Fiúza, 1984; Alvarez-Salgado et al., 2003) affect the site. Subtropical ENACW is generally upwelled south of 40° N and subpolar one north of 45° N. In between either water mass can be upwelled depending on the

strength of the wind forcing. Strong winds can cause subpolar ENACW to be upwelled also south of 40° N. In the deep, all sites are currently bathed by North Atlantic Deep Water (NADW) that at site MD03-2699 is slightly modified due to the entrainment of the warmer and more saline Mediterranean Outflow Water (MOW).

Outside of the western Iberian upwelling region plankton blooms drive surface water productivity (Levy et al., 2005; Table 1). Site MD01-2446 falls within the mid-latitude regime that is associated with a bloom that starts in fall and peaks in spring. The northern boundary of this regime is at $40\pm2°$ N, so that IODP Site U1313 either follows this regime or experiences a major late spring bloom and a smaller fall bloom like it is typical for the subpolar regime and for ODP Site 980. ODP Sites 1056 and 1058, on the other hand, follow the subtropical regime with a weak fall bloom.

3 Methods

Sediment samples for stable isotope and lithics analyses of IODP Site U1313 and cores MD03-2699 and MD01-2446 were prepared in LNEG's Laboratorio de Geologia Marinha following the established procedure. After freeze drying samples were washed with deionized water through a 63 µm-mesh and the coarse fraction residue was dried in filter paper at 40 °C and weighted. Sample intervals are 1–3 cm for core MD03-2699 and 2–3 cm for core MD01-2446. IODP Site U1313 was sampled continuously with 2 cm-wide scoops. Site U1313 stable isotope samples were taken from the secondary splice and biomarker samples from the primary splice (Stein et al., 2009).

For planktic stable isotope measurements in cores MD03-2699 and MD01-2446 and IODP Site U1313, 8–10 clean specimens of *Globorotalia inflata* were picked from the fraction >315 µm and not treated further prior to analysis. *G. inflata* is one of the dominant species in the planktic foraminifer fauna associated with the NAC (Ottens, 1991). Its stable isotope values reflect hydrographic conditions at the base of the seasonal thermocline (Cléroux et al., 2007); conditions that are close to those in the winter mixed layer to which Ganssen (1983) relates *G. inflata* in the NW-African upwelling region. Details on stable isotope measurements for ODP Site 980 are given by Oppo et al. (1998) and McManus et al. (1999), for ODP Site 1056 by Chaisson et al. (2002) and Billups et al. (2004) and for ODP Site 1058 by Billups et al. (2006). Because of laboratory offsets ODP Site 1056 *N. dutertrei* δ^{18}O values needed to be adjusted by +0.2‰ in order to match absolute values of ODP Site 1058.

Benthic isotope records of cores MD03-2699 and MD01-2446 and IODP Site U1313 are based on 2–4 clean specimens of *Cibicidoides wuellerstorfi*, *Cibicidoides mundulus* or *Cibicidoides pachyderma* (the latter only in MD03-2699). At few levels where *C. wuellerstorfi* was absent *Uvigerina* sp. was picked instead. All *Cibicidoides* sp. δ^{18}O data is corrected by +0.64‰ to the *Uvigerina* sp. level (Shackleton, 1974). Benthic and planktic stable isotope samples were measured in a Finnigan MAT 252 mass spectrometer at Marum (University Bremen, Germany). The mass spectrometer is coupled to an automated Kiel carbonate preparation system and the long-term precision is ±0.07‰ for δ^{18}O and ±0.05‰ for δ^{13}C based on repeated analyses of internal and external (NBS-19) carbonate standards.

The number of lithic fragments was determined in the fraction >315 µm and is presented as "#/g" (normalized by the respective sample's dry weight). Lithics are primarily interpreted as IRD. The coarser size fraction was chosen 1) to minimize modification of the IRD signal by wind deposition and lateral advection at slope site MD03-2699 and 2) to avoid scientific overlap for Site U1313 within the science party of IODP Exp. 306. Using a coarser size fraction allows to identify all the ice-rafting events (e.g., Voelker, 1999) and only this is relevant for the current study, but might underestimate the absolute intensity of an ice-rafting event.

Biomarker samples of IODP Site U1313 and core MD03-2699 were prepared following established procedures (Villanueva et al., 1997; Calvo et al., 2003). Core MD03-2699 samples were analysed in a Varian gas chromatograph either at the Dept. of Environmental Chemistry of CSIC (Barcelona) or at the Unidade de Geologia Marinha of LNEG (Rodrigues et al., 2010). Site U1313 samples were measured in a gas chromatograph/time-of-flight mass spectrometer at the Alfred-Wegner Institute, Bremerhaven (Hefter, 2008; Stein et al., 2009). Alkenone-based sea surface temperatures (SST) for both sites were calculated using the unsaturation index $U_k^{37'}$ of Müller et al. (1998) and thus reflect annual mean SST.

IODP Site U1313, MD01-2446 and MD03-2699 data is stored at the World Data Centre Mare and can be accessed through the following parent link: http://doi.pangaea.de/10.1594/PANGAEA.742794.

4 Chronostratigraphy

Ages for most of the cores are derived from the LR04 stack (Lisiecki and Raymo, 2005). The benthic record of IODP Site U1313, the re-occupation of DSDP Site 607, was directly correlated with the stack with most correlation points being isotopic maxima. The record of MD01-2446 was correlated with the Site U1313 curve in the interval where the two overlap and to the LR04 stack for the interval from late MIS 10 to MIS 9. The resulting records are shown in Fig. 2a and their age/depth relations in Fig. 2c.

Establishing the age model for intermediate depth site MD03-2699 was more difficult as the deep water δ^{18}O signal here is strongly modified by the MOW during glacials and glacial inceptions (Voelker et al., 2007). Except for one point, the age model for this core is based on the correlation of its benthic δ^{18}O record to the one of ODP Site 980 (on

Table 2. Age model, sedimentation rates and relevant nannofossil events for core MD03-2699.

Depth (cm)	Age (ka)	Sedimentation rate (cm/ky)	Comment
1135	301.54	5.46	Correlation of primary signals
1158	305.75	5.15	Correlation of primary signals
1205	314.88	3.68	Alignment of minima
1245	325.76	4.46	Alignment
1270	331.36	2.48	Correlation of primary signals
1293	340.64	5.40	Correlation of primary signals
1428	365.66	5.15	Alignment of peaks
1468	373.42	5.13	Correlation of primary signals
1520	383.55	6.05	Correlation of primary signals
1559	390.00	8.68	Correlation of primary signals
1636	398.87	6.50	Alignment
1662	402.87	6.06	Alignment
1711	410.96	7.40	Correlation of primary signals
1803	423.40	7.42	Alignment of minima
1849	429.60	1.91	Correlation of primary signals
1861	435.87	2.05	Alignment
1895			LCO of *P. lacunosa* (Amore et al., 2010)
1938	473.48	4.95	Correlation of primary signals
2034	492.88	5.23	Correlation of primary signals
2123	509.90	9.33	Alignment of end of MIS 13b cold event in *G. inflata* records of cores MD03-2699 and U1313
2170			FO of *H. inversa* (Amore et al., 2010)
2258	524.37	11.55	Correlation of primary signals
2393	536.06	10.94	Correlation of primary signals
2407	537.34	4.75	Correlation of primary signals
2450			Onset of *G. caribbeanica* acme (Amore et al., 2010)
2483	553.33		Correlation of primary signals

LR04 time) and three nannofossil events (Table 2). ODP Site 980 was chosen as reference curve over the LR04 stack as it is from intermediate water depths too. Consequently, water mass signals during times of lower MOW influence at site MD03-2699 were similar at both sites (Fig. 2b). To establish the age model clear signals in both records were correlated first, the primary control points (Table 2). As second step, signals that were already nearly in phase based on the first correlation, were aligned. Three nannofossil events (Amore et al., 2010; Table 2) corroborate the age model: the acme of *Gephyrocapsa caribbeanica* (Flores et al., 2003; Baumann and Freitag, 2004); the first occurrence of *Heliosphaera inversa* within MIS 13 (514.9 ka); and the last common occurrence (LCO) of *Pseudoemiliania lacunosa*. The *G. caribbeanica* acme begins in late MIS 14 (546.4 ka) and helps to constrain the core's basal age. The LCO of *P. lacunosa* is placed at the depth of 1895 cm equal to an age of 452.5 ka, in agreement with the zone for the LCO defined by Raffi et al. (2006).

Due to stronger winnowing by the MOW as evidenced by foraminifer sands, sedimentation rates in core MD03-2699 subsided during glacial maxima, especially during MIS 12 (Table 2; Fig. 2c). Overall, sedimentation rates of core MD03-2699 and IODP Site U1313 are similar, while they are lower in core MD01-2446 (Fig. 2c). Temporal resolution of the stable isotope records are 100–600 years for IODP Site U1313, 90–1210 years for core MD03-2699 and 280–1820 years for core MD01-2446.

ODP Site 980 records are shown on the LR04 age model of Lisiecki and Raymo (2005) in this paper and the *N. pachyderma* (*r*) stable isotope records have a temporal resolution of 40 to 3230 years. The age scale of ODP Site 1056 was transferred to LR04 time using the Billups et al. (2004) correlation points between ODP Sites 1056 and 980 (placed on LR04 time). For ODP Site 1058 we are using the alternative age model of Weirauch et al. (2008) that correlates ODP Site 1058 with ODP Site 677, as this age model results in a better agreement between hydrographic conditions at (I)ODP Sites 1058 and U1313 during MIS 14. Temporal resolution of the *N. dutertrei* stable isotope records varies between 110 to 1830 years for ODP Site 1056 and 40 to 2260 years in ODP Site 1058.

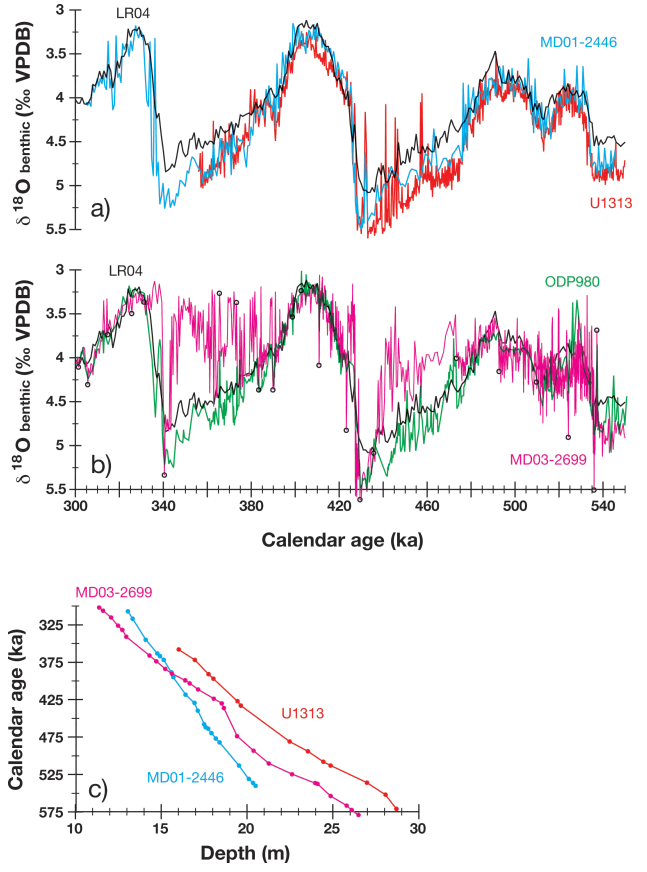

Fig. 2. **(a)** Benthic δ^{18}O records of IODP Site U1313 (red) and MD01-2446 (cyan) in comparison to the LR04 stack (black) (Lisiecki and Raymo, 2005); **(b)** Benthic δ^{18}O record of MD03-2699 (magenta) in comparison to ODP site 980 (green; on LR04 timescale) and the LR04 stack (black). Black circles on the MD03-2699 record mark age control points (Table 2). **(c)** Age-depth relationships for IODP Site U1313 and cores MD01-2446 and MD03-2699.

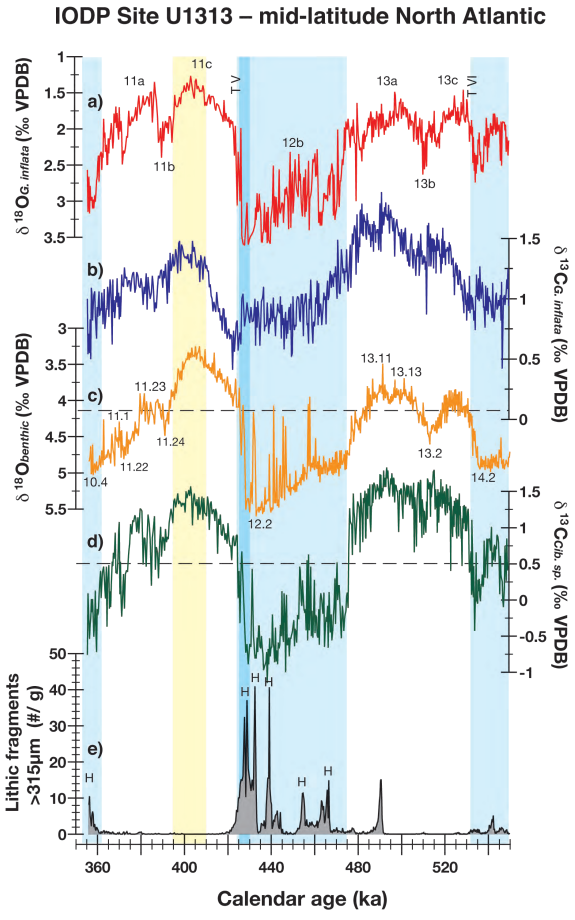

Fig. 3. Records for IODP Site U1313 in the mid-latitude North Atlantic (34: a) *G. inflata* δ^{18}O (‰VPDB; red), b) *G. inflata* δ^{13}C (‰VPDB; blue), c) benthic δ^{18}O (‰VPDB; orange), d) epibenthic δ^{13}C (‰VPDB; green), and e) lithics concentration (#/g; black). Light blue bars mark glacial MIS 10, 12 and 14; dark blue bar the Heinrich-type event at the end of MIS 12; and the yellow bar the MIS 11 sea level highstand. Substages (e.g. 11c) are indicated on the *G. inflata* δ^{18}O record (a) and isotopic events (e.g. 10.4) on the benthic δ^{18}O record (c). Dashed line in c) designates the ice volume threshold of McManus et al. (1999) and in d) the NADW/Antarctic Bottom Water boundary. T IV, V and VI refer to Terminations VI, V and VI. H indicates IRD peaks with Heinrich-type signatures (Stein et al., 2009).

5 Results

5.1 IODP Site U1313

The record of IODP Site U1313 (Fig. 3) spans the interval from 550 to 355 ka fully capturing interglacial MIS 13 and MIS 11 as well as the MIS 14 to 13 deglaciation (Termination VI). MIS 13 and 11 both contain pronounced cooling events that separate intervals of peak warmth (δ^{18}O < 1.75‰). *G. inflata* and benthic δ^{18}O values show the familiar glacial to interglacial variations with lowest values between 417 and 396 ka, i.e. during MIS 11c. Similarly, MIS 13 contains two warm stages, MIS 13c and 13a, with lowest planktic δ^{18}O values recorded during the early stages. Other than during the distinct cooling events, the range of individual planktic δ^{18}O fluctuations is relatively small in comparison to the pronounced δ^{18}O variability during glacial MIS 12. Termination V is the one of the largest glacial to interglacial transition of the middle Pleistocene while Termination VI is probably one of the smallest (Lisiecki and Raymo, 2005). The benthic and planktic δ^{18}O values of IODP Site U1313 decreased ∼1.5‰ and 1‰, respectively. Both events, however, reveal a reversal toward higher planktic δ^{18}O values midway through the transition, similar to the Younger Dryas during the last Termination.

Although MIS 11c may have been the warmest interval of the past 1000 ka, both δ^{13}C records contain a maximum in the later stage of MIS 13 (MIS 13a; Fig. 3b and d). High δ^{13}C values are a typical signal for mid-Brunhes planktic and

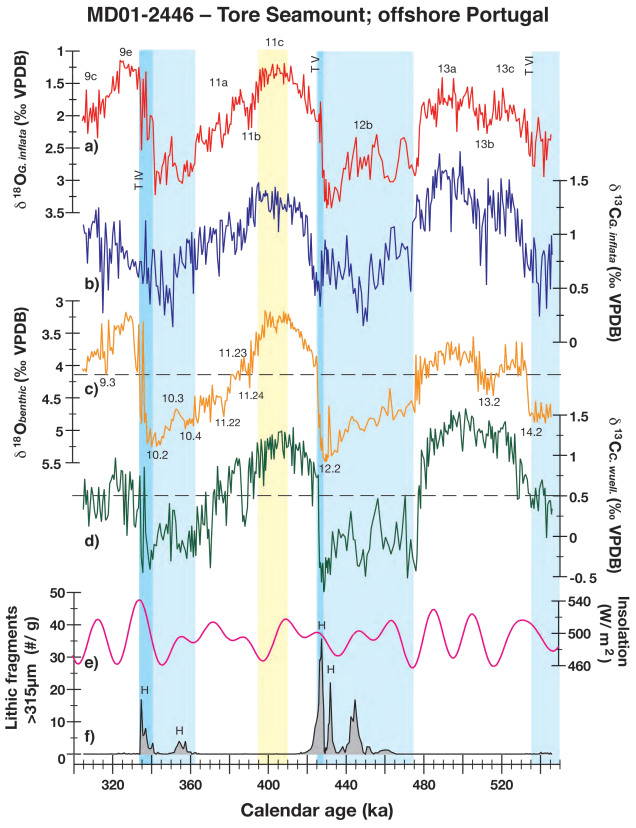

Fig. 4. Records for core MD01-2446, the offshore site off Portugal: **(a)** *G. inflata* δ^{18}O (‰VPDB; red), **(b)** *G. inflata* δ^{13}C (‰VPDB; blue), **(c)** benthic δ^{18}O (‰VPDB; orange), **(d)** epibenthic δ^{13}C (‰VPDB; green), **(e)** 21 June insolation at 65° N (Laskar et al., 2004; magenta), and **(f)** lithics concentration (#/g; black). Light blue bars mark glacial MIS 10, 12 and 14; dark blue bars the Heinrich-type events at the Terminations; and the yellow bar the MIS 11 sea level highstand. Substages (e.g. 11c) are indicated on the *G. inflata* δ^{18}O record (a) and isotopic events (e.g. 10.4) on the benthic δ^{18}O record (c). Dashed line in c) designates the ice volume threshold of McManus et al. (1999) and in d) the NADW/Antarctic Bottom Water boundary. T IV, V and VI refer to Terminations VI, V and VI. H indicates Heinrich-type ice-rafting events.

benthic δ^{13}C records (Fig. 3d and 4d; Hodell et al., 2003; Wang et al., 2003). During MIS 13c and 11c, *G. inflata* δ^{13}C values were at a similar level, but on average 0.5‰ lower than during MIS 13a. Terminations VI and V were associated with pronounced δ^{13}C minima. Deep water ventilation (benthic δ^{13}C; Fig. 3d) was similar during MIS 13c, 13a and 11c and increased immediately at the Terminations preceding the (sub)surface waters. During the interstadials of late MIS 11 and of MIS 14, benthic δ^{13}C values indicated the presence of NADW and thus a strong AMOC. This relationship did, however, not exist during MIS 12 when higher benthic δ^{13}C values often coincided with lower planktic δ^{18}O values (Fig. 3a and d).

Melting icebergs reached IODP Site U1313, located within the area of high IRD sedimentation during Heinrich events (Hemming, 2004), during all the mid-Brunhes glacials, but IRD deposition was more pronounced and frequent during MIS 12 (Fig. 3e). The first IRD event recorded at site U1313 during the transition from MIS 13 to 12 occurred at 490 ka followed by a 23 ka long period with continuous, but not intense IRD sedimentation. After 467 ka, the record reveals four intervals of increased IRD deposition with the last interval exhibiting three short-term maxima. All IRD maxima as well as the IRD peak during MIS 10 (isotopic event 10.4) contain dolomite grains (Stein et al., 2009) and are thus interpreted as Heinrich-type ice-rafting events. During MIS 13a IRD deposition ceased for 12 ka (506.4–494.3 ka). During Termination V continuous IRD deposition ended already at 415.9 ka and during MIS 11c melting icebergs did not reach Site U1313 between 410.7 and 399.6 ka (Fig. 6b).

5.2 Core MD01-2446

The *G. inflata* δ^{18}O record of core MD01-2446, the offshore site off Portugal, shows the same features as the Site U1313 record with relative stable conditions during the interglacials and millennial-scale variability during glacial inceptions and glacials (Fig. 4a). In contrast to Site U1313 conditions in the thermocline waters were more variable during MIS 13 and cooling during MIS 13b was less. The interval with values $<$1.75‰ during MIS 11c lasted from 419.4 until 395.6 ka or even 394.3 ka, if one excludes the short excursion down to 1.8‰ at 395.3 ka. During MIS 9e, such light isotope values are observed continuously between 335 and 317 ka. MIS 11c and 9e δ^{18}O values were in the same range and even some values during MIS 13a reached this level (Fig. 4a). The MD01-2446 record shows several δ^{18}O oscillations during Terminations VI and IV, while the Termination V sequence looks similar to the Site U1313 record but with less pronounced cooling during the Heinrich-type ice-rafting event. Also MD01-2446's benthic δ^{18}O record is in general similar to the one of Site U1313 (Fig. 4c).

Analogous to the Site U1313 records, *G. inflata* and benthic δ^{13}C was highest during MIS 13a and values during MIS 13c and 11c were in a similar range. In contrast, planktic and benthic δ^{13}C values during interglacial MIS 9e were much lower and kept on rising during the interglacial to reach maximum values only during MIS 9d (Fig. 4b and d). Glacial planktic δ^{13}C minima were lower than at Site U1313 and glacial benthic δ^{13}C in the same range or higher. In contrast to Site U1313, *G. inflata* recorded a pronounced δ^{13}C minimum between 452 and 443 ka offshore Portugal. During MIS 10, lower planktic δ^{13}C values occurred especially between 351 and 342 ka.

Although Site U1313 received continuous but in comparison to the other glacials small amounts of IRD during MIS 14 (Fig. 3e), (coarse) IRD deposition offshore Portugal was

nearly negligible and no IRD was deposited during MIS 13 after 523 ka (Fig. 4f). During MIS 12, melting icebergs started to reach the Portuguese margin after 472 ka, i.e. significantly later than at IODP Site U1313. The last two IRD peaks in core MD01-2446 during MIS 12 coincided with the last interval of increased IRD deposition at Site U1313 and its Heinrich-type IRD events. At site MD01-2446, however, IRD deposition greatly diminished between the Heinrich-type events. During MIS 10, phases of intensive ice rafting coincided with stadial MIS 10c and with Termination IV. Minor amounts of lithic grains, generally clear quartz grains, were deposited throughout MIS 9e (Fig. 4f), especially until 322 ka. However, as the tropical planktic foraminifer species *G. menardii* is found in the same samples as the quartz grains and mean annual SST further south on the margin exceeded 18 °C (Martrat et al., 2007) these grains were more likely deposited by strong westerly winds during the upwelling season than by melting ice. During MIS 11c, coarse lithics were not deposited between 410.8 and 393.6 ka with the exception of one quartz grain found at 404.2 ka that was probably also wind-transported. After 393.6 ka minor amounts of lithics were encountered throughout the glacial inception.

During the millennial-scale oscillations of the glacial inceptions warmer/colder conditions in the surface water (lower/higher *G. inflata* δ^{18}O values) were contemporary with a better/poorer ventilation of the deep waters bathing site MD01-2446 (Fig. 4a and e), similar to the AMOC patterns during the MIS 3 interstadial/stadial cycles (Shackleton et al., 2000).

5.3 Core MD03-2699

At nearshore site MD03-2699 the glacial to interglacial pattern that is so clearly evident at the other two sites is more difficult to detect. While glacial maxima of MIS 12 and 10 are recorded as distinct δ^{18}O maxima and interglacials as distinct minima (Fig. 5a and c), glacial inceptions are characterized by relatively large δ^{18}O variability masking a clear designation into substages. Furthermore, large fluctuations (>0.5‰) in the planktic δ^{18}O values are evident during the early stages of MIS 13 (MIS 13c). In fact, Termination VI is entirely masked by high amplitude δ^{18}O variations, and the MIS 13 stadial event (isotopic event 13.2) sees a return to glacial-like δ^{18}O values. Warmer thermocline temperatures (δ^{18}O < 1.75‰) dominated during interglacial MIS 11c between 417 and 394.7 ka and during MIS 9e from 336.2 to 319 ka. The single or double point δ^{18}O maxima recorded during MIS 11c were confirmed by duplicate analyses and the accompanying δ^{13}C values are not analytical outliers. None of the other available high-resolution proxy records for the core (e.g., biomarkers, Corg, carbonate, XRF-Sr, % reworked coccolith species, various planktic foraminifer stable isotope and trace element records; Rodrigues et al., 2010; Amore et al., 2010; Salgueiro et al., unpubl. data) show any deviations from the surrounding interglacial levels making

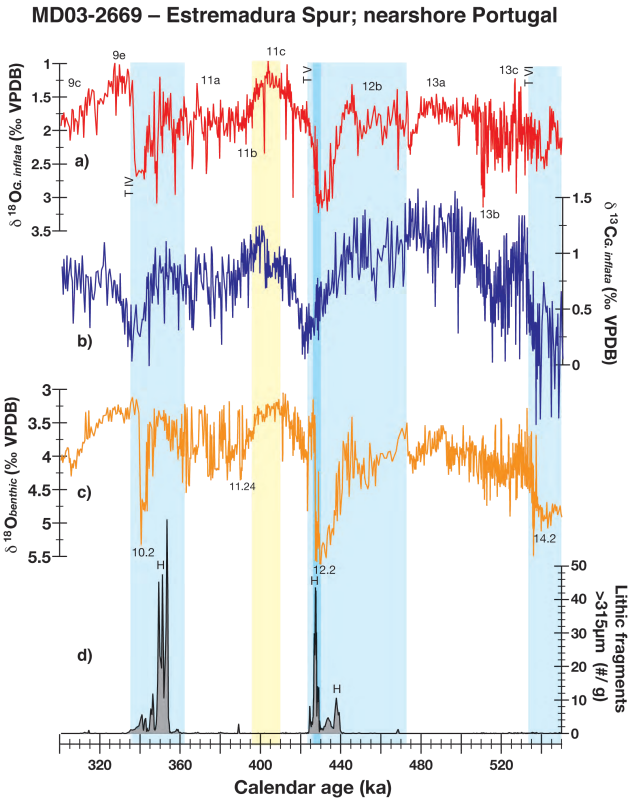

Fig. 5. Records for core MD03-2699, the nearshore site off Portugal: **(a)** *G. inflata* δ^{18}O (‰VPDB; red), **(b)** *G. inflata* δ^{13}C (‰VPDB; blue), **(c)** benthic δ^{18}O (‰VPDB; orange), and **(d)** lithics concentration (#/g; black). Light blue bars mark glacial MIS 10, 12 and 14; dark blue bar the Heinrich-type event at the end of MIS 12; and the yellow bar the MIS 11 sea level highstand. Substages (e.g. 11c) are indicated on the *G. inflata* δ^{18}O record (a) and isotopic events (e.g. 10.4) on the benthic δ^{18}O record (c). T IV, V and VI refer to Terminations VI, V and VI. H indicates Heinrich-type ice-rafting events.

reworking or core disturbances at or around those levels also an unlikely source. Thus the *G. inflata* values are seen as to be correct and appear to reflect the presence of very cold wintertime thermocline waters.

All three glacial inceptions reveal millennial-scale oscillations (Fig. 5a and c) and planktic δ^{18}O values remained relatively low until the subsequent glacial maximum was reached. Planktic values during the warm phases of these oscillations were in the range of the MIS 13a levels, especially during MIS 12. Also values during interstadial MIS 14b (isotopic event 14.3) reached such levels. During MIS 9d and 9c, thermocline δ^{18}O values (temperatures) were as low (warm) as during MIS 13a or the warm oscillations recorded during MIS 12b and 10b.

Overall, the shape of the planktic δ^{13}C record (Fig. 5b) mimics the pattern described for IODP Site U1313 and site MD01-2446 with highest δ^{13}C values recorded during MIS

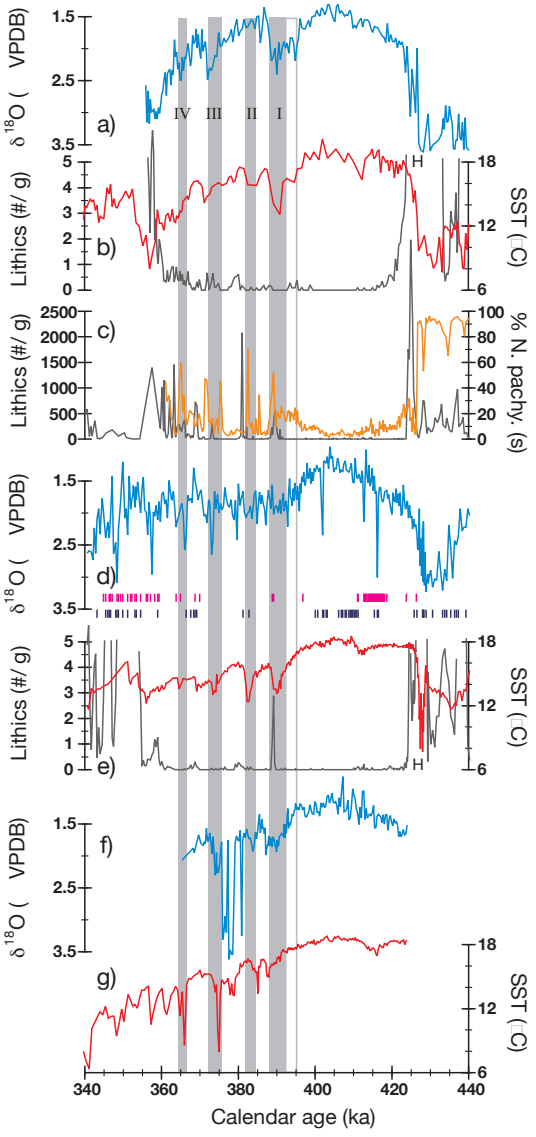

Fig. 6. Close-ups of MIS 11 in the records of IODP Site U1313 (**a** and **b**), ODP Site 980 **(c)**, MD03-2699 (**d** and **e**) and southern Portuguese site MD01-2443 (**f**, **g**; (de Abreu et al., 2005; Martrat et al., 2007)). *G. inflata* δ^{18}O records are shown in blue (a, d, f), alkenone-based mean annual sea surface temperature (SST) records in red (b, e, g). The abundance of Lithics $>315\,\mu$m (gray; only sections with <5 grains/g) are shown for IODP Site U1313 (b) and core MD03-2699 (e) and $>150\,\mu$m for ODP Site 980 (c; Oppo et al., 1998). Panel c) also includes the % *N. pachyderma* (s) record of ODP Site 980 (orange; Oppo et al., 1998). In panel d) magenta bars indicate presence of *Globorotalia menardii* and dark blue ones of *Sphaeroidinella dehiscens* in the respective levels. MD01-2443 data is shown using the age model of Tzedakis et al. (2009) that links the MD01-2443 benthic δ^{18}O data to the EDC δD record on the EDC 3 timescale (Jouzel et al., 2007) following the approach of Shackleton et al. (2000). Grey bars indicate stadials (numbered I to IV) within MIS 11a. The bar outlined in grey during the oldest stadial marks the interval when cold conditions already prevailed at (I)ODP Sites U1313 and 980. H denotes the Heinrich-type ice-rafting event associated with Termination V.

13 and 11. Contrary to those records high δ^{13}C values persisted throughout much of MIS 12. The same is seen during the MIS 10 inception and early MIS 10. Similar to site MD01-2446 interglacial MIS 9e is associated with increasing δ^{13}C values that reached higher levels only during MIS 9d and 9c. During MIS 11c the δ^{13}C record shows a stepwise recovery from the minimum during Termination V. The first "plateau" with values generally between 0.75 and 0.9‰ lasted from 416 to 401.6 ka, followed by a second maximum with values mainly between 1 and 1.25‰ from 401.3 to 395 ka. Also the MIS 13 record of MD03-2699 shows more structure than in the previous records. Although highly variable, early MIS 13c is associated with a maximum in δ^{13}C values, followed by a broad minimum lasting from late MIS 13c to MIS 13b and a subsequent maximum with the highest values (up to 1.47‰) recorded at site MD03-2699 during MIS 13a. The lowest δ^{13}C values of the record were recorded during the colder phases of MIS 14.

Trace amounts of lithics $>315\,\mu$m were found during MIS 14, early MIS 13c and MIS 13b (Fig. 5d). During MIS 12 the first, but minor IRD peak occurred at 468.8 ka. Continuous IRD deposition started after 442 ka and lasted until 423.3 ka. IRD peaks during this interval coincided with the Heinrich-type events recorded at IODP Site U1313. After this interval with intensive IRD deposition, minor amounts of lithics (mainly quartz grains) were detected until 410 ka. In three levels during MIS 11c (Fig. 6e) 1 or 2 quartz grains were observed, but these grains are most likely wind-transported from the Portuguese coast. A significant IRD peak occurred around 389 ka within MIS 11b (isotopic event 11.24; Figs. 5 and 6e). After this first MIS 11 stadial, minor amounts of lithics were deposited on and off throughout MIS 11a (Fig. 6e). As all those periods of lithic grain deposition coincided with the presence of tetra-unsaturated alkenones (Rodrigues et al., 2010), which are linked to fresher surface waters (Bard et al., 2000), the lithics are interpreted as IRD. MIS 10 is associated with another extended period (363–333.4 ka) of ice rafting.

5.4 Sea surface temperature reconstructions for MIS 10 to 12

Annual mean SST at IODP Site U1313 varied between 7.7 and 20.2 °C (Fig. 6b). The coldest SST was recorded during the Heinrich-type ice-rafting events of MIS 12 and isotopic event 10.4. SST rose quickly after the onset of Termination V increasing by nearly 8.5 °C between 427 and 423 ka. During MIS 11c two SST plateaus with values around 18 °C are observed with the second plateau, which also experienced minimally warmer SST, coinciding with the interglacial sea level highstand (408–396 ka). During the subsequent glacial inception, the more pronounced cooling occurred during the MIS 11b stadial (isotopic event 11.24; ∼390 ka).

At core site MD03-2699 mean annual SST were relatively warm during MIS 12 with 11.7 to 15.8 °C (Fig. 6e). SST

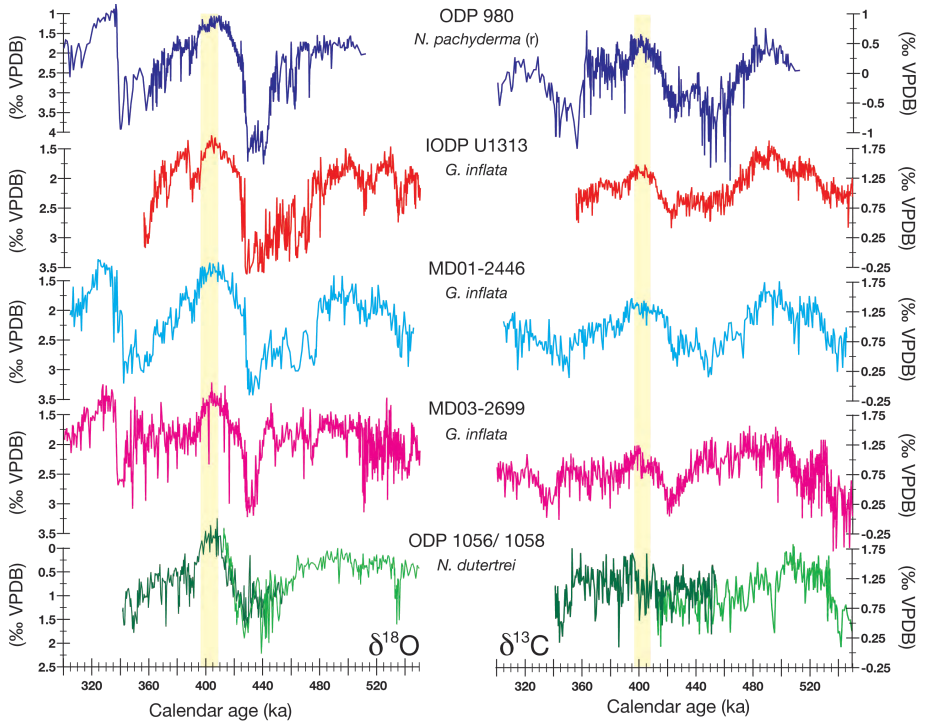

Fig. 7. North Atlantic planktic foraminifer stable isotope records with δ^{18}O records on the left and δ^{13}C records on the right. Sites are arranged from North to South: ODP Site 980 (dark blue), IODP Site U1313 (red), MD01-2446 (light blue), MD03-2699 (magenta), and ODP Sites 1056 (dark green) and 1058 (light green) combined. Yellow bars highlight the period of the MIS 11c sea level highstand.

then dropped to values below 8 °C during the Heinrich-type event at the beginning of Termination V. Similar to the *G. inflata* δ^{13}C records the SST data also shows two plateaus for MIS 11c. The first plateau with SST around 17.6 °C lasted from 425.5 to 414.8 ka, followed until 410.1 ka by an interval with more variable SST and some values as low as 16.8 °C. The second SST plateau with values exceeding 18 °C lasted from 410.1 to 402.9 ka, but SST dropped permanently below 17.5 °C only after 397.2 ka with the transition into stadial MIS 11b. During the MIS 10 inception, the SST record reveals four cold/warm cycles whose amplitude weakened towards MIS 10d (Fig. 6e). MIS 10b was associated with warmer SST that were as warm as the warm oscillations within MIS 11a.

5.5 Comparison to published records

North Atlantic ODP Site 980's δ^{18}O data was discussed in previous publications (Oppo et al., 1998; McManus et al., 1999) and is shown in Fig. 7. This site's δ^{13}C record of *N. pachyderma* (*r*) reveals the lowest δ^{13}C values during the earliest phase of MIS 12 and during the colder intervals of MIS 10 (Fig. 7). δ^{13}C levels recorded during interglacials MIS 13a and 11c were similar and about 0.5‰ heavier than those during interglacial MIS 9e. With the onset of the inception of glacial MIS 12 (480 ka), δ^{13}C values declined continuously towards the MIS 12b minimum (isotopic event 12.2). During the inception of glacial MIS 10, on the other hand, δ^{13}C values remained relatively high between 390 and 360 ka; levels that frequently exceeded the MIS 9e values. The inception of MIS 10 is nevertheless modified by higher frequency variability.

For western subtropical Atlantic ODP Sites 1056/1058 the *N. dutertrei* stable isotope records are also shown in Fig. 7. *N. dutertrei* records conditions towards the bottom of the seasonal thermocline (Billups et al., 2004) with the highest flux in winter (Deuser and Ross, 1989). Thus its living conditions are comparable to those of *G. inflata* (Fairbanks et al., 1980; Deuser and Ross, 1989; Cléroux et al., 2007). Contrary to the other sites in this study, heaviest δ^{13}C values were not concurrent with the sea level highstands of MIS 13a and 11c, both of which exhibit relatively low values (Fig. 7). Times with highest δ^{13}C values coincided with late MIS 14 to 13c and with stadial MIS 11b. For most of the record covered by Site 1056 (MIS 12–10; darker green line in Fig. 7), δ^{13}C values varied between 0.75 and 1.5‰ and dropped to a longer lasting minimum only during the glacial maximum of MIS 10. Thus there was no major difference between glacial MIS 12 and warm MIS 11. A similar pattern is seen at ODP Site 1058 where interglacial MIS 13a and higher values during glacial MIS 12 reached comparable levels (lighter green line in Fig. 7). However, δ^{13}C values declined from MIS 13a to the MIS 12 glacial maximum, despite of millennial-scale variability overprinting the record.

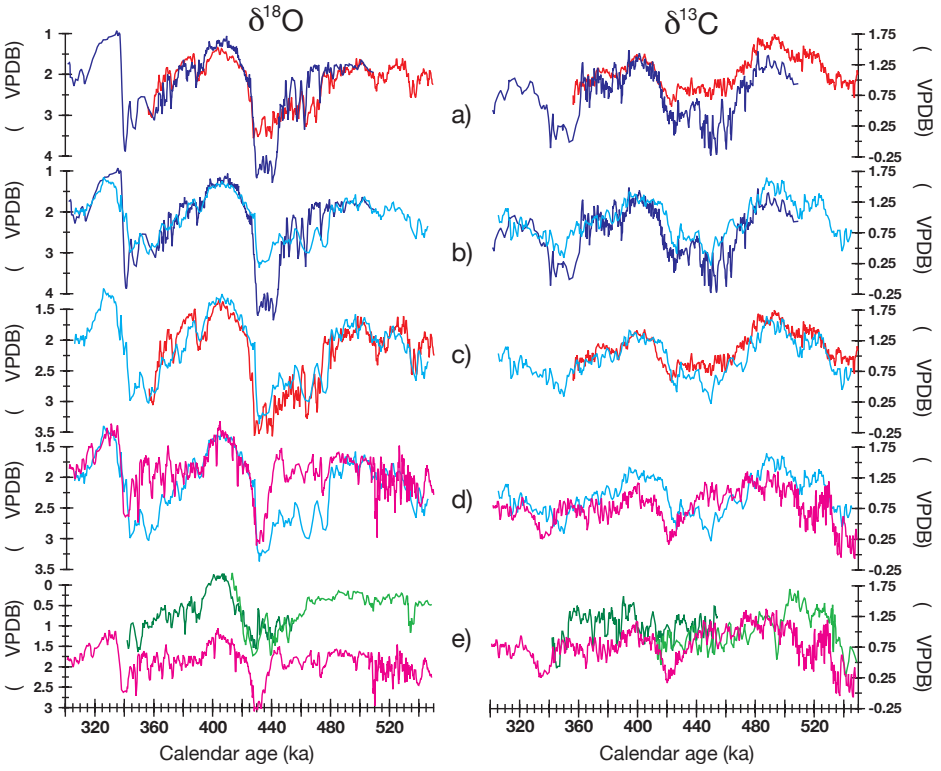

Fig. 8. Direct comparison between sites based on 3 point average records (δ^{18}O left, δ^{13}C right side). Colors for sites as in Fig. 7. **(a)** IODP Site U1313 vs. ODP Site 980. For better comparison ODP Site 980 *N. pachyderma* (*r*) δ^{13}C data was adjusted to dissolved inorganic carbon (DIC) by adding 0.85‰ (Labeyrie and Duplessy, 1985). **(b)** MD01-2446 vs. ODP Site 980 (with δ^{13}C adjusted); **(c)** MD01-2446 vs. IODP Site U1313; **(d)** MD01-2446 vs. MD03-2699; **(e)** ODP Sites 1056 and 1058 vs. MD03-2699.

6 Discussion

6.1 Hydrographic conditions off Portugal

Although core sites MD03-2699 and MD01-2446 are located only about 170 km apart, their *G. inflata* δ^{18}O records are very different in that the nearshore site displays large and rapid fluctuations suggesting very different hydrographic conditions, especially during the glacial inceptions and glacials. The two sites are more similar during interglacial MIS 9e, 11c and 13a, but with core MD03-2699 revealing slightly lower values, thus indicating warmer waters (Figs. 7 and 8). We suggest that the higher variability in the planktic δ^{18}O and δ^{13}C records of core MD03-2699 reflects variations in upwelling of deeper waters into the thermocline. Increased productivity during MIS 13, especially during MIS 13c, the first half of MIS 11c and the inception of MIS 10 is clearly indicated by the maxima in total alkenone concentration and Corg (Rodrigues et al., 2010). While the interglacial δ^{18}O levels are similar at the two sites and for MIS 11c also in agreement with those recorded for core MD01-2443 (Fig. 6f; de Abreu et al., 2005), *G. inflata* δ^{13}C values at site MD01-2446 are generally higher (Fig. 8d) indicating that more nutrients were available in the offshore waters either because of lower nutrient consumption (open ocean vs. upwelling regime) or because the waters offshore had already higher preformed nutrient concentrations.

The alkenone-derived SST (Fig. 6e) indicates extremely stable mean annual surface water temperatures during MIS 11c in the nearshore waters off Portugal. The MD03-2699 record agrees well with the one of core MD01-2443 (Fig. 6g; Martrat et al., 2007). Both show two plateaus within MIS 11c and a short minimum prior to the second, warmer plateau coinciding with the MIS 11c sea-level highstand (note that the minimum in MD01-2443 is shifted towards older ages with the Tzedakis et al. (2009) age model (Fig. 6g), while with the de Abreu et al. (2005) age model (not shown) the minima are aligned). Such a SST stability over thousands of years is not seen in the NAC waters at IODP Site U1313 (Fig. 6b) where temperatures, nevertheless, reveal the same three phased pattern and reached values similar to those off Portugal. More variable conditions in the NAC waters were probably linked to admixing of subpolar surface waters, especially during the first MIS11c temperature plateau when hydrographic conditions in the Nordic Seas (Helmke and Bauch, 2003) and the Arctic Ocean (Knies et al., 2007), thus in the subpolar and polar regions, were still unstable due to freshwater release. Less stable conditions in the

AMOC during the first half of MIS 11c are also indicated by the benthic δ^{13}C records for IODP Site U1313 and MD01-2446 (Figs. 3d and 4d) that reveal that deep water ventilation, while already at NADW level, still increased and experienced short periods with lesser ventilation. The SST stability off Portugal, on the other hand, must be related to a dominant influence of the subtropical AzC and IPC waters and thus confirm that the hydrographic (winter-time) situation off Portugal during MIS 11c was comparable to the Present (Figs. 1b and 9a). This is further supported by faunal evidence. Tropical planktic foraminiferal species contributed significantly to the MIS 11c fauna of core MD01-2443 (de Abreu et al., 2005) and the deeper dwelling tropical species *Globorotalia menardii* and *Sphaeroidinella dehiscens*, both of which do not occur in the modern fauna off western Iberia (Salgueiro et al., 2008), were found in MIS 11c and 9e samples of cores MD03-2699 (Fig. 6d) and MD01-2446. Consequently, both the surface and subsurface poleward flows in the North Atlantic's eastern boundary system – with a higher contribution of tropical waters than today – transported heat northward during those periods.

MIS 11c interglacial conditions in the surface and deep waters off Portugal ended around 395 ka with the onset of the 11b stadial (isotopic event 11.24; Figs. 4 and 5). At the Iberian margin, cooling during this stadial was gradual and coldest conditions were reached only towards the end of the stadial coincident with IRD maxima around 389 ka (Figs. 4 and 6) and concurrent with pollen evidence from core MD01-2447 (42° N; Desprat et al., 2005). Although site MD03-2699 received more IRD, δ^{18}O-inferrred surface water-cooling seems to have been similar at the two sites (Fig. 8d). Because the MD01-2443 record, located just about one degree further to the south, reveals less cold temperatures (Fig. 6), subtropical AzC waters probably still influenced the southern margin, similar to the stadials and Heinrich events of the last glacial cycle (Salgueiro et al., 2010), and their presence might have enhanced iceberg melting near site MD03-2699. The arrival of IRD at the Iberian margin and thus the southernmost position of the Polar Front in the eastern North Atlantic coincided with the strongest reduction in the AMOC as indicated by the benthic δ^{13}C minima in the IODP Site U1313 and MD01-2446 records (Figs. 3d and 4d) that lasted from 389 to 387 ka and was more pronounced in the eastern basin (MD01-2446). The Site U1313 records, however, reveal that ventilation in the deep western boundary current (DWBC) already started to decline with the onset of IRD deposition (Fig. 3).

MIS 11a and thus the glacial inception of MIS 10 is marked by three interstadial/stadial cycles, the first interstadial of which is associated with isotopic event 11.23 (Figs. 3–6). During this interstadial surface waters in the North Atlantic started to warm after 388 ka (Figs. 3–7), while AMOC strength was still reduced (Figs. 3d and 4d). Cooling during the second stadial is much stronger on the northern (Desprat et al., 2005) and middle Iberian margin (MD03-2699) than in the NAC waters (IODP Site U1313). Therefore a European or Scandinavian source for the cooling is more likely than advection with the NAC from the western subpolar gyre, the typical source region for MIS 3 ice-rafting events. Such an eastern source region is supported by the stronger IRD signal at ODP Site 980 (Fig. 6c; Oppo et al., 1998) than at IODP Site U1313, even given the differences in the IRD size fraction, and in agreement with modelling results (Bigg et al., 2010). During early MIS 10, the presence of tropical foraminifer species (Fig. 6d) again indicate a strengthening of the eastern boundary undercurrent that could explain why mean annual SST and the winter mixed layer at site MD03-2699 were hardly impacted by the Heinrich-type event during isotopic event 10.4, even though melting icebergs reached site MD03-2699 (Figs. 5 and 6e) and the Polar Front had moved to a more southern position as consequence of the reduced AMOC (indicated by the low benthic δ^{13}C values at Site U1313 and MD01-2446; Figs. 3d and 4d).

With the onset of MIS 11a the *G. inflata* δ^{18}O and δ^{13}C records of core MD03-2699 start to diverge from the offshore signal at site MD01-2446 (Fig. 8d). For most of the glacial inception, δ^{18}O values in core MD03-2699 stayed low, while values in core MD01-2446 increased as is to be expected with gradual cooling and increasing ice volume. The difference between these two relative closely located core sites can only be caused by a strong hydrographic front. Because *G. inflata* is reflecting winter mixed-layer conditions this front must have been the northward trending subtropical front, in a manner similar to the Present (Fig. 1b–d). The strong IPC influence on the southwestern margin is confirmed by the *G. inflata* δ^{18}O values and warm SST of core MD01-2443 (Fig. 6f and g; de Abreu et al., 2005), which, with the exception of the unusually high values between 375 and 381 ka, have levels similar to those of core MD03-2699. The signal at offshore site MD01-2446, on the other hand, agrees well with the NAC record of IODP Site U1313 (Fig. 8c) and therefore in the PC's source waters. The northward extending subtropical front and thus the dominant IPC influence on nearshore waters off Portugal persisted into the glacial. Only during those times when *G. inflata* δ^{18}O values in core MD03-2699 became temporarily higher and reached MD01-2446 levels (Fig. 8d), like during stadials II and III, did the front not exist and colder waters also penetrated into the nearshore regions.

For the transition from MIS 13a to 12a four short-term colder episodes are detected in the *G. inflata* δ^{18}O record of core MD03-2699. Values during those times did, however, not reach the colder MD01-2446 levels (Fig. 8d), except for the short IRD event at 470 ka (Fig. 5) that like stadial MIS 11b also had more likely an eastern source because a pronounced IRD peak is recorded at site M23414 (Kandiano and Bauch, 2003; Fig. 1a) and ODP Site 980 (Oppo et al., 1998) but not at IODP Site U1313 (Fig. 3e). Overall, wintertime hydrographic conditions in the nearshore waters off Portugal appear to have been warmer and more stable during MIS 12 than during the subsequent glacial inception. Such

temperature "stability" points to a strong AzC influence and is conform to evidence from the western Mediterranean Sea where planktic δ^{18}O records of ODP Sites 976, 977 and 975 (Pierre et al., 1999; von Grafenstein et al., 1999) reveal significantly warmer surface waters during glacial MIS 12 and 14 than during MIS 10. The strong AzC influence resulted in SST at site MD03-2699 rising continuously towards the deglaciation (Fig. 6e). As consequence a SST gradient of $\geq$5 °C existed between IODP Site U1313 and MD03-2699 indicating that a front – either just the subtropical front off Portugal or even the subpolar front – separated the surface waters in this mid-latitudinal band; not much different from the last glacial maximum (Calvo et al., 2001; Pflaumann et al., 2003). The deglacial SST rise off Portugal was, however, abruptly interrupted by the significant cooling associated with the Heinrich-type ice-rafting event around 427 ka (Hodell et al., 2008; Stein et al., 2009). This Heinrich-type event had a major impact on the North Atlantic's hydrography, even leaving a freshwater signal in the *G. inflata* records of core MD01-2446 (low δ^{18}O values contemporary with light δ^{13}C values; Fig. 4a and b), and led to a temporary AMOC shut down as revealed by the benthic δ^{13}C records of IODP Site U1313 and MD01-2446 (Figs. 3d and 4d), just like its younger counterparts.

The pattern with a strong subtropical front separating sites MD03-2699 and MD01-2446 and with subtropical AzC/IPC waters dominating the Portuguese nearshore waters is thus a recurrent feature – also seen during MIS 14 and the glacial inception starting with stadial MIS 9d (Fig. 8d) – during the glacial inceptions and glacials of the mid-Brunhes period. It seems, however, to be linked more to eastern boundary system dynamics than to the AMOC because warming and cooling cycles were generally the same at both sites (Figs. 7 and 8d) and higher IPC influence at site MD03-2699 coincided with periods of higher upwelling-related productivity (Rodrigues et al., 2010).

6.2 Basinwide circulation and linkages to thermocline water sources

Both the PC and the IPC also have a subsurface component of subpolar or subtropical waters, respectively, whose properties contribute to those in the deep winter mixed layer in which deeper dwelling foraminifer like *G. inflata* calcify their tests. By tapping into subsurface waters deep winter mixing replenishes the nutrients available in the upper water column. Since δ^{13}C values measured in planktic foraminifer tests are related to nutrient concentrations (Broecker and Peng, 1982; Ortiz et al., 1996) we are using them to trace the subsurface/mode waters in the North Atlantic. Such an approach is facilitated by the fact that the subpolar mode water is formed during winter along the NAC branches around the Rockall Plateau (Brambilla and Talley, 2008) and thus in close vicinity to ODP Site 980. Because the mode water is directly advected southward with the PC the transport way is relatively short minimizing the time during which the δ^{13}C signal could be modified. Furthermore, the selected planktic foraminifer species represent conditions in winter and thus prior to the spring blooms and upwelling season during which the δ^{13}C would be altered due to nutrient consumption. The comparison between sites focuses on trends and not on absolute values because the δ^{13}C values of the different species were not corrected to dissolved inorganic carbon (DIC) levels (except for the ODP Site 980 *N. pachyderma* (*r*) values in Fig. 8a and b where the correction was added to minimize the plot's δ^{13}C range). Thus only the δ^{13}C values of the *G. inflata* based records of IODP Site U1313, MD01-2446 and MD03-2699 are directly comparable.

In the direct comparison it becomes clear that the offshore core MD01-2446 is very similar to IODP Site U1313 (Figs. 7 and 8c) indicating that for most of the studied interval hydrographic conditions, i.e. temperature and salinity properties, were not much different in the NAC and the PC, most likely facilitated by the spreading of the subpolar mode water (e.g., during MIS 11c, Fig. 9a). For most of the time the *G. inflata* δ^{13}C values at both sites were comparable and generally heavier than at site MD03-2699. However, there were also intervals when the two open ocean records diverged. One such example is the interstadial associated with isotopic event 11.23 when warm conditions in the NAC at IODP Site U1313 lasted longer than in the PC record of core MD01-2446 that is more comparable with the NAC record at ODP Site 980 (Figs. 7, 8a–c). Thus it might be that the NAC's main flow path was shifted more southward than its current position (Fig. 1a) and that the NAC waters reaching the Rockall Plateau and feeding the PC were already modified by entrainment of subpolar waters. The more southern NAC path could be linked to the less stable AMOC conditions already mentioned above. A strong linkage in water mass conditions between the Rockall Plateau NAC branch and the PC is confirmed by the planktic δ^{13}C records (Figs. 7 and 8b). This relationship is especially evident during MIS 12 when the MD01-2446 δ^{13}C data follows the ODP Site 980 record, especially the pronounced δ^{13}C minimum during early MIS 12 that is only recorded at these two sites (Fig. 7). Thus it appear that the poorly ventilated surface to subsurface waters advected southward with the PC during MIS 12 were formed near or above the Rockall Plateau, probably in regions similar to those of modern subpolar mode water formation (Brambilla and Talley, 2008; Fig. 9b). MIS 12 δ^{13}C values at IODP Site U1313, on the other hand, stayed fairly constant despite the strong temperature and salinity oscillations indicated by the δ^{18}O data and the presence of melting icebergs (Fig. 3). Thermocline waters in this region were better ventilated than in the eastern basin indicating that Gulf Stream waters (ODP Site 1056 and 1058; Fig. 7) still reached this latitude (Fig. 9b), in agreement with the relative warm SST during most of MIS 12 (Stein et al., 2009). The influence of these Gulf Stream derived NAC waters was diminished in the eastern basin and they had hardly any impact on

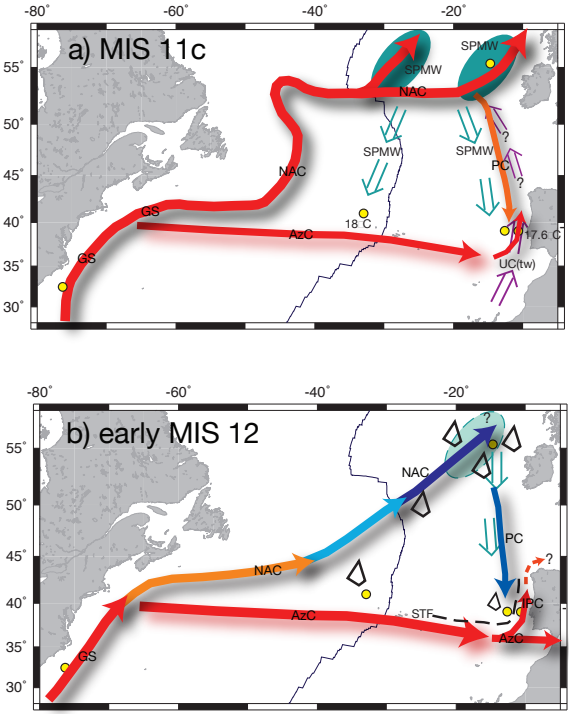

Fig. 9. Circulation schemes for interglacial MIS 11c **(a)** and early glacial MIS 12 **(b)** arising from this study. Abbreviations for currents are the same as in Fig. 1. Open arrows show subsurface flows. UC(tw) indicates undercurrent transporting tropical waters and SPMW subpolar mode waters formed in the regions designated by ellipses of the same color. SST values listed in (a) give means for the interval from 425 to 396 ka for the alkenone temperatures measured at IODP Site U1313 and in core MD03-2699. Dashed line in (b) indicates (winter-time) hydrographic front separating sites MD01-2446 and MD03-2699, here denoted as subtropical front (STF). Black "diamonds" indicate presence of melting icebergs based on IRD data and include evidence from core M23414 (Kandiano and Bauch, 2003) and from IODP Site U1308 (Hodell et al., 2008).

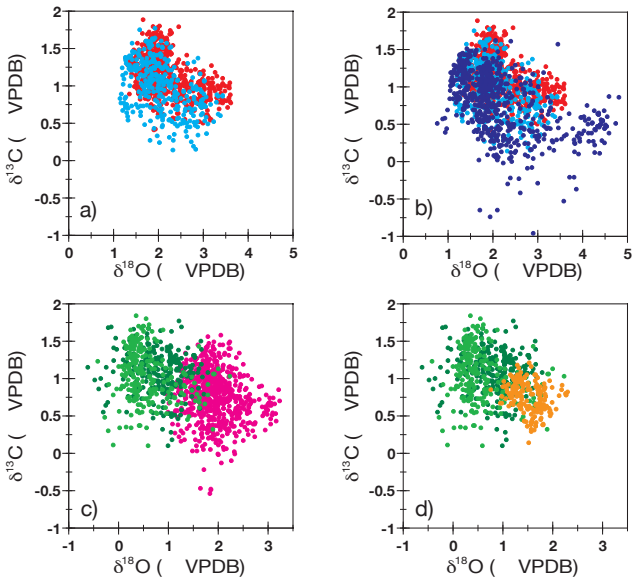

Fig. 10. δ^{18}O versus δ^{13}C scatter plots of the records shown in Fig. 7. **(a)** IODP Site U1313 (red) and MD01-2446 (light blue); **(b)** IODP Site U1313 (red), MD01-2446 (light blue), and ODP Site 980 (dark blue); **(c)** MD03-2699 (magenta) and ODP Sites 1056 (dark green) and 1058 (light green); **(d)** ODP Sites 1056 (dark green) and 1058 (light green) and MD01-2443 (orange; de Abreu et al. (2005); with extreme values between 375 and 381 ka excluded).

the AMOC because the benthic δ^{13}C values (Figs. 3d and 4d) indicate a strong presence of Southern Sourced Waters. Especially during early MIS 12, the position of the Polar Front appears to have been tilted in the North Atlantic reaching further to the south in the eastern than western basin. The glacial differences are also well seen in the scatter plots (Fig. 10a) with divergences towards higher/lower δ^{13}C values in IODP Site U1313 and core MD01-2446, respectively. However, these plots also reveal that during most of the time, in particular during the interglacial intervals (lower δ^{18}O values), conditions at the three sites influenced by the NAC and PC were not much different (Fig. 10b); thus making the NAC like today the dominant hydrographic feature in the mid-latitude North Atlantic.

Although the NAC and PC records at IODP Site U1313, ODP Site 980 and site MD01-2446 agree well, there is one interval when the MD01-2446 record diverges from the others and this is the planktic δ^{13}C minimum associated with Termination V (Fig. 8a–c). During the onset of the deglaciation δ^{13}C levels are similar at the three sites. However, while the δ^{13}C minimum at Site U1313 lasted for 10 ka, which is similar to ODP Site 980 (Fig. 8a), at site MD01-2446 it ended after only 5 ka, which is also sooner than at site MD03-2699 (Fig. 8d). The late glacial and deglacial δ^{13}C minima, previously described by Spero and Lea (2002) for Southern Hemisphere waters, are generally linked to poorly ventilated and thus nutrient-rich water masses such as Subarctic Intermediate Water (Venz et al., 1999) or Antarctic Intermediate Water like in the Spero and Lea (2002) study, the latter of which penetrated as far north as 61.5° N during the last deglaciation (Rickaby and Elderfield, 2005). The presence of better ventilated waters at site MD01-2446 therefore implies the formation of well ventilated mode water, perhaps similar to the formation of subtropical ENACW along the Azores front nowadays, somewhere south of 41° N and offshore of western Iberia. In contrast to the surface waters the deep water ventilation increased immediately and abruptly after the Heinrich-type event of Termination V indicating the presence of NADW at the two deeper sites and a stronger AMOC right at the onset of MIS 11c (Figs. 3 and 4). This decoupling between the surface and deep water ventilation raises

the question where in the North Atlantic did deep convection occur, and we suggest the well ventilated NADW recorded in both basins originated north of the studied core sites (e.g. Nordic Seas??). A different duration of the deglacial planktic δ^{13}C minimum is not seen for Termination VI, when it lasted about 8 ka at both IODP Site U1313 and site MD01-2446. By contrast the timing of deep water ventilation changes differed in the two basins because the DWBC at Site U1313 (Fig. 3d) already transported well ventilated NADW southward while ventilation in the eastern basin increased more slowly (Fig. 4d). Also at Termination IV more poorly ventilated surface to subsurface waters were present in the eastern North Atlantic basin (ODP Site 980, MD01-2446, MD03-2699; Fig. 8b and d) and the minimum lasted for almost 20 ka, i.e. well into the interglacial setting MIS 9e apart from other interglacial intervals. This difference is not only evidenced by the prolonged planktic δ^{13}C minimum but also by the persistent, if low presence of the polar species *N. pachyderma* (s) in the planktic foraminifer fauna off Iberia during the first half of the interglacial (de Abreu et al., 2005; Desprat et al., 2009) implying the advection of poorly ventilated waters into the mid-latitude North Atlantic. These waters were most likely Subarctic Intermediate Water because the record of ODP Site 982 on the northern Reykjanes ridge (57.5° N) reveals the same δ^{13}C minimum accompanied by persistent, but low input of IRD (Venz et al., 1999). The persistent influx of less saline arctic surface waters to the deep water convection areas could also explain the high variability in AMOC strength depicted in the benthic δ^{13}C data of core MD01-2446 (Fig. 4d).

As already mentioned above the planktic δ^{13}C values in records for NAC and PC waters were mostly higher than at site MD03-2699 in agreement with subpolar source waters being better ventilated than subtropical ones. Given that the δ^{18}O and SST data implies a strong AzC/IPC influence on the latter record, the δ^{13}C values of core MD03-2699 should show some resemblance to those values recorded in the subtropical Gulf Stream waters at ODP Sites 1056 and 1058 (Figs. 7 and 8e). Based on the scatter plots (Fig. 10c and d) there is only minor overlap between the records from the western and eastern side of the North Atlantic basin and that seems mainly to be restricted to MIS 11 as implied by the MD01-2443 data (Fig. 10d). The *N. dutertrei* δ^{13}C record of ODP Site 1056 shows a similar pattern to core MD03-2699 during MIS 11c with lower values indicating relatively more nutrients during the early phase and higher values during the later phase of the interglacial (Fig. 8e). Consequently, this two-step feature in nutrient concentrations is a subtropical gyre signal. Trends and even absolute δ^{13}C values were also similar at ODP Sites 1056 and 1058 and site MD03-2699 between 495 and 440 ka and after 350 ka (Fig. 8e); thus during those glacial times, when SSTs and δ^{18}O data of core MD03-2699 indicate a strong subtropical water influence. The good correspondence during MIS 12 might indicate that cross-Atlantic transport with the AzC was strong with little admixing of transitional waters (Fig. 9b); in agreement with the western Mediterranean Sea evidence mentioned in 6.1. During the inception of MIS 10, nutrient concentrations at site MD03-2699 were higher than at ODP Site 1056 indicating that the Gulf Stream waters were greatly modified before reaching the western Iberian margin, if they contributed to the subsurface waters there at all. The δ^{13}C records between the two sites also diverged during MIS 13c and b, when upwelling from either subtropical or subpolar ENACW influenced site MD03-2699. The records were also decoupled during the glacial maximum of MIS 12, when the subtropical front did not separate waters at site MD03-2699 from those recorded in core MD01-2446 and subpolar waters influenced the western Iberian margin.

6.3 Comparison of the interglacials

The new records from the mid-latitude North Atlantic confirm MIS 11c to be a long and relative stable interglacial in comparison to either MIS 13 or MIS 9 in regard to both the surface and deep water circulation. Especially the NAC and PC waters experienced only minor changes in the hydrographic conditions and nutrient levels. Thus conditions in the mid-latitude North Atlantic were comparable to those of ODP Site 980 (Oppo et al., 1998; McManus et al., 2003). Based on the δ^{18}O records hydrographic conditions in those waters were also stable during MIS 9e, while MIS 13c and 13a experienced some small-scale oscillations and consequently less stable conditions (Fig. 7). MIS 13c and 13a are also confirmed to have been colder than the subsequent interglacials with only short intervals during MIS 13a reaching δ^{18}O values comparable to MIS 11c or 9e levels (Figs. 4a–6a). In the sites affected by subtropical waters (ODP Sites 1056 and 1058; MD03-2699) variability in the surface water properties was slightly higher during MIS 11c and 9e than in the NAC and PC records, while MIS 13 appears more stable in the Gulf Stream waters (Figs. 7 and 8e). At site MD03-2699, on the other hand, MIS 13c and 13a were quite different. Hydrographic conditions during MIS 13c were highly variable due to intense upwelling (see Sect. 6.1), but were more stable and comparable to ODP Site 1058 during MIS 13a (Fig. 8e).

Overall, MIS 11c and 9e appear to have experienced comparable temperature and salinity conditions in the mid-latitude North Atlantic surface waters. However, there is one major difference and that is the ventilation of the surface to subsurface waters and their impact on the AMOC. While no impact of the poorly ventilated and potentially fresher waters during MIS 9e is seen in the planktic δ^{18}O records presented here, they affected the ventilation of the lower NADW as reflected in the MD01-2446 (Fig. 4d) and IODP Site U1308 (Hodell et al., 2008) records. Because the upper NADW as recorded at ODP Site 980 (McManus et al., 1999) was well ventilated, only the deeper branch was affected – either because the Iceland-Scotland Overflow Water (ISOW) exiting

from the Nordic Seas was poorly ventilated or AMOC was shallower during early MIS 9e. Anyhow, a shallower AMOC or poorly ventilated ISOW sets MIS 9e apart from MIS 11c, when the AMOC strengthend at the onset of the interglacial. During MIS 13c, deep water ventilation was more variable than during MIS 11c, especially in the DWBC (Fig. 3d), while conditions during MIS 13a were again comparable.

The new records extend the region with stable temperature conditions during MIS 11c down to 39° N and confirm that overall hydrographic conditions and circulation pathways in the North Atlantic basin were similar to today. In addition, the following new insights into hydrographic conditions in the subtropical gyre could be gained:

1. the existence of two SST plateaus with the second period experiencing slightly warmer temperatures and coinciding with the sea level highstand and both associated with the AMOC in the interglacial mode;

2. increased northward heat flux of subsurface tropical waters with the eastern boundary undercurrent, especially during the early phase of MIS 11c;

3. a two step evolution in planktic δ^{13}C indicating poorer ventilated subtropical waters during the early phase and better ventilated ones during the second phase; the transition in δ^{13}C occurred during the sea level highstand and thus later than the transition to warmer SST;

4. the formation of well ventilated mode waters in the vicinity of core MD01-2446 during the transition from glacial MIS 12 to interglacial MIS 11c.

These new results have implications on the numerical modelling of interglacial intervals. Our records provide regional-scale data for peak interglacial warmth of MIS 11c. For example models may incorporate two temperature plateaus during MIS 11c, the first one being the colder one, setting MIS 11c apart from younger interglacial periods such as MIS 9e or MIS 5e, when warmest SST were recorded at the beginning of the interglacial (e.g., McManus et al., 1999; Martrat et al., 2007). Furthermore, the increased subsurface heat transport with the undercurrent needs to be accounted for and balanced within the AMOC. The question still remains what is driving this enhanced transport. Stronger deep convection in the North Atlantic, which could explain why these waters potentially reached site M23414 at the Rockall Plateau (Kandiano and Bauch, 2007; Fig. 9a)? And/or is the undercurrent replacing surface waters exported from the western Iberian margin during upwelling? Strong winds reconstructed off NW Africa by Helmke et al. (2008) would induce enhanced upwelling during the first phase of MIS 11c, in agreement with the productivity data from core MD03-2699 (Rodrigues et al., 2010). The lower planktic δ^{13}C values in core MD03-2699 indicate upwelling of nutrient poorer water and, if nutrient poorer and relative warmer waters were upwelled all along the Iberian margin, productivity must have been lower than today, especially off Galicia, and this would affect the carbon cycle. So while current pathways and the North Atlantic's thermohaline circulation overall were similar between MIS 11c and the Holocene (McManus et al., 1999; Rodrigues et al., 2010) and not much different during MIS 13a and 13c, our results show that one should not neglect the details and that the differences revealed by these details need to be accounted for, also in future climate modeling studies. Due to the dual nature of the subsurface circulation and heat fluxes transient models might actually be needed to fully understand MIS 11c climate evolution. However, prior to modeling, the amount of heat advected northward needs to be better quantified, because, while our data allows us to reconstruct the transport pathways, we cannot quantify the amount, yet. The regions where the well ventilated NADW was convected at the beginning of MIS 11c also still need to be specified.

7 Conclusions

By combining the records of six core sites spanning the latitudes from 32 to 55.5° N and the major surface water currents linked to the subtropical and transitional waters in the North Atlantic Ocean we are able to trace hydrographic conditions from MIS 9 to 14. Overall, planktic foraminiferal δ^{18}O values and alkenone derived SSTs indicate that surface water temperature and salinity conditions during the interglacials MIS 11c and MIS 9e were not much different and very stable along the NAC and PC. During MIS 9e, surface water ventilation was relatively poor and this signal was transported down into the AMOC's deeper branch. On the other hand, enhanced northward transport of tropical waters within the eastern boundary undercurrent is observed during MIS 11c and MIS 10 off Portugal. This observation raises the question as to the mechanisms driving this heat flux and how these waters may have affected productivity off Iberia. During early MIS 11c the northward advected (sub)tropical waters even reached the Rockall Plateau (Kandiano and Bauch, 2007) and thus the regions where subpolar mode water is formed today. Based on our results subpolar mode water was also formed in that region in the past and was one of the signal carriers linking hydrographic conditions in the subpolar North Atlantic and the transitional waters recorded in the mid-latitudes at IODP Site U1313 and site MD01-2446. Our results also show for the first time that along with the enhanced northward heat flux hydrographic conditions in the offshore waters off Portugal were such that well ventilated mode waters were formed during the glacial to interglacial transition. So far these mode waters have only been recorded at site MD01-2446 and it remains to be seen in the future if their impact was locally restricted and if they might have been formed in polynia-type open waters. Since this is also the time when ventilation in the surface waters was delayed relative to the deep waters, future studies need to pinpoint where the lower

NADW originated from. In agreement with previous observations in the North Atlantic MIS 13 is revealed as colder than the younger interglacial intervals. Due to strong upwelling during MIS 13c the planktic isotope records of core MD03-2699 experienced pronounced variability, while conditions during MIS 13a were relative stable and comparable to those in the Gulf Stream. Overall, it appears that conditions in the mid-latitude North Atlantic were not much different during MIS 11c than during MIS 9e and, if one neglects the generally lower temperatures, also during MIS 13a. Current pathways in the surface and deep ocean and associated fronts were similar to today during all the interglacials. The difference between the interglacials lies in the ventilation of the subsurface waters and the subsurface heat flux. Here MIS 9e stands apart because of the continuous admixing of poorly ventilated arctic waters into the transitional waters of the mid-latitude North Atlantic and MIS 11c because of the enhanced subsurface heat flux during the slightly colder first phase.

Based on the closely spaced core sites MD03-2699 and MD01-2446 we could also show for the first time that a strong hydrographic front existed off Portugal, especially during the glacial inceptions and glacials. This front appears to have been equal to the northward extending subtropical front that exists during modern winters (Figs. 1b and 9b). East of the front, i.e. in the nearshore waters off Portugal, a strong influence of subtropical AzC waters is recorded at sites MD03-2699 and MD01-2443. Accordingly, the pronounced SST stability recorded in these waters during MIS 11c might be more typical for the subtropical gyre than a Gulf Stream/NAC signal. Future records off NW Iberia and off NW Africa, i.e. up- and downstream, might help to shed some light onto this question. The hydrographic front disappeared sporadically during stadials of the glacial inception of MIS 10, but cooling episodes in the nearshore waters were much shorter than those recorded offshore (Figs. 7 and 8d). Since the flow of the subtropical waters was poleward future studies need to solve how far north the associated heat was felt, because if they entered the Bay of Biscaye they would have affected the ice sheets reaching the Armorican and Celtic margins and could have facilitated some of the "Fleuve Manche" mass transport events observed by Toucanne et al. (2009).

Increased heat transport with the AzC across the Atlantic, even into the Mediterranean Sea, is also seen during MIS 12 when δ^{13}C records of ODP Sites 1056 and 1058, representing Gulf Stream waters, and of core MD03-2699 were most similar (Fig. 8e). Differing from the younger glacials depicted in the MD01-2443 record (Martrat et al., 2007), the alkenone SST record of core MD03-2699 confirms relative warm waters at this site and warming from the glacial maximum to the interglacial would probably have been continuously if it had not been interrupted by a Heinrich-type ice-rafting event. Cooling during this event is comparable to the cooling observed during younger Heinrich events (e.g. de Abreu et al., 2003). While the nearshore waters off Portugal had a subtropical source during MIS 12, the offshore waters were derived from the Rockall Plateau region as the close correspondence between the records of ODP Site 980 and core MD01-2446 reveal (Figs. 8b and 9b). The surface waters in the eastern basin were poorer ventilated than those in the western basin (IODP Site U1313), even though the western basin experienced stronger salinity oscillations linked to more frequent ice-rafting events. Thus during most of MIS 12 NAC waters still reached IODP Site U1313, confirmed by the SST record (Stein et al., 2009), but did not enter into the eastern basin. Consequently, during MIS 12 the position of the Polar Front was tilted reaching further south in the eastern basin and coming in close contact with the subtropical front off Portugal. By comparing the records from the different regions it became evident that climate evolution in the western and eastern basin can differ depending on the NAC strength or the source region for melting icebergs and that more than one site is needed for a comprehensive picture.

For the better understanding of interglacial climates we could show that circulation patterns did not differ from today. However, if we want to fully understand similarities and differences between MIS 11c and the Holocene or even future climate at minimum regional-scale climate models need to incorporate some of our findings regarding heat transport pathways and ventilation because they in return affected the AMOC, even if we might not yet fully understand their impacts.

Acknowledgements. This study used samples provided by the Integrated Ocean Drilling Program (IODP) and by the British Ocean Sediment Core Research Facility (BOSCOR). The Fundação para a Ciência e a Tecnologia (FCT) through the PORTO (PDCT/MAR/58282/2004) and SEDPORT projects (PDCTM/40017/2003), and postdoctoral (SFRH/BPD/21691/2005) and PhD (SFRH/BP/13749/2003) fellowships funded A. V. and T. R. Additional funding to T. R. and J. G. was provided by the Consolider-Ingenio 2100 Project CE-CSD2007-0067. Coring of MD03-2699 was made possible through a European Access to Research Infrastructure grant. We thank IPEV, Yvon Balut and the captain and crews of R/V Marion Dufresne for their support in retrieving the two Calypso cores. Special thanks go to Monika Segl (Marum, University Bremen) for the measuring of the isotope samples, to Lucia de Abreu for sampling core MD01-2446, and to Miguel Reis of the ITN in Lisbon for access to the freeze dryer in his lab. The staff of the DGM lab and J. P. Ferreira and B. Montanari are greatly appreciated for their support in sampling and sample preparation. U. Paczek, M. Ferreira, B. Montanari and C. Trindade helped with the picking of some of the stable isotope samples.

Edited by: P. Tzedakis

References

Alvarez-Salgado, X. A., Figueiras, F. G., Perez, F. F., Groom, S., Nogueira, E., Borges, A. V., Chou, L., Castro, C. G., Moncoiffe, G., and Rios, A. F.: The Portugal coastal counter current off NW Spain: new insights on its biogeochemical variability, Prog. Oceanogr., 56, 281–321, 2003.

Amore, F. O., Flores, J. A., Voelker, A. H. L., Lebreiro, S., and Sierro, F. J.: Coccolithophore record during the middle Pleistocene in the North Atlantic: paleoclimatic and paleoproductivity patterns, Mar. Micropaleontol., submitted, 2010.

Bard, E., Rostek, F., Turon, J.-L., and Gendreau, S.: Hydrological Impact of Heinrich Events in the Subtropical Northeast Atlantic, Science, 289, 1321–1324, 2000.

Barker, S., Archer, D., Booth, L., Elderfield, H., Henderiks, J., and Rickaby, R. E. M.: Globally increased pelagic carbonate production during the Mid-Brunhes dissolution interval and the CO_2 paradox of MIS 11, Quaternary. Sci. Rev., 25, 3278–3293, 2006.

Bauch, H. A., Erlenkeuser, H., Helmke, J. P., and Struck, U.: A paleoclimatic evaluation of marine oxygen isotope stage 11 in the high-northern Atlantic (Nordic seas), Global Planet. Change, 24, 27–39, doi:10.1016/S0921-8181(99)00067-3, 2000.

Baumann, K.-H. and Freitag, T.: Pleistocene fluctuations in the northern Benguela Current system as revealed by coccolith assemblages, Mar. Micropaleontol., 52, 195–215, doi:10.1016/j.marmicro.2004.04.011, 2004.

Berger, W. H. and Wefer, G.: On the Dynamics of the Ice Ages: Stage-11 Paradox, Mid-Brunhes Climate Shift, and 100-ky Cycle, in: Earth's Climate and Orbital Eccentricity: the Marine Isotope Stage 11 Question edited by: Droxler, A. W., Poore, R. Z., and Burckle, L. H., Geophysical Monograph, American Geophysical Union, Washington, DC, 41–59, 2003.

Bigg, G. R., Levine, R. C., Clark, C. D., Greenwood, S. L., Haflidason, H., Hughes, A. L. C., Nygård, A., and Sejrup, H. P.: Last glacial ice-rafted debris off southwestern Europe: the role of the British-Irish Ice Sheet, J. Quaternary. Sci., 25(5), 689–699, doi:10.1002/jqs.1345, 2010.

Billups, K., Chaisson, W., Worsnopp, M., and Thunell, R.: Millennial-scale fluctuations in subtropical northwestern Atlantic surface ocean hydrography during the mid-Pleistocene, Paleoceanography, 19(2), PA2017, doi:10.1029/2003PA000990, 2004.

Billups, K., Lindley, C., Fisler, J., and Martin, P.: Mid Pleistocene climate instability in the subtropical northwestern Atlantic, Global Planet. Change, 54, 251–262, 2006.

Brambilla, E. and Talley, L. D.: Subpolar Mode Water in the northeastern Atlantic: 1. Averaged properties and mean circulation, J. Geophys. Res., 113, C04025, doi:10.1029/2006JC004062, 2008.

Broecker, W. S. and Peng, T.-H.: Tracers in the Sea, Tracers in the Sea, ELDIGIO Press, Lamont-Doherty Geological Observatory, Columbia University, Palisades, New York, 690 pp., 1982.

Calvo, E., Villanueva, J., Grimalt, J. O., Boelaert, A., and Labeyrie, L.: New insights into the glacial latitudinal temperature gradients in the North Atlantic. Results from Uk37' sea surface temperatures and terrigenous inputs, Earth Planet. Sc. Lett., 188, 509–519, 2001.

Calvo, E., Pelejero, C., and Logan, G. A.: Pressurized liquid extraction of selected molecular biomarkers in deep sea sediments used as proxies in paleoceanography, J. Chromatogr. A, 989, 197–205, 2003.

Chaisson, W. P., Poli, M.-S., and Thunell, R. C.: Gulf Stream and Western Boundary Undercurrent variations during MIS 10-12 at Site 1056, Blake-Bahama Outer Ridge, Mar. Geol., 189, 79–105, 2002.

Channell, J. E. T., Kanamatsu, T., Sato, T., Stein, R., Alvarez Zarikian, C. A., Malone, M. J., and the Expedition 303/306 Scientists: Proceedings IODP, 303/306, Integrated Ocean Drilling Program Management International, Inc., College Station TX, 2006.

Chapman, M. R. and Maslin, M. A.: Low-latitude forcing of meridional temperature and salinity gradients in the subpolar North Atlantic and the growth of glacial ice sheets, Geology, 27, 875–878, 1999.

Cléroux, C., Cortijo, E., Duplessy, J.-C., and Zahn, R.: Deep-dwelling foraminifera as thermocline temperature recorders, Geochem. Geophy. Geosy., 8, Q04N11, doi:10.1029/2006GC001474, 2007.

de Abreu, L., Shackleton, N. J., Schoenfeld, J., Hall, M., and Chapman, M.: Millennial-scale oceanic climate variability off the Western Iberian margin during the last two glacial periods, Mar. Geol., 196, 1–20, 2003.

de Abreu, L., Abrantes, F. F., Shackleton, N. J., Tzedakis, P. C., McManus, J. F., Oppo, D. W., and Hall, M. A.: Ocean climate variability in the eastern North Atlantic during interglacial marine isotope stage 11: a partial analogue to the Holocene?, Paleoceanography, 20, PA3009, doi:10.1029/2004PA001091, 2005.

Desprat, S., Sanchez Goñi, M. F., Turon, J. L., McManus, J. F., Loutre, M. F., Duprat, J., Malaize, B., Peyron, O., and Peypouquet, J. P.: Is vegetation responsible for glacial inception during periods of muted insolation changes?, Quaternary Sci. Rev., 24, 1361–1374, 2005.

Desprat, S., Sánchez Goñi, M. F., McManus, J. F., Duprat, J., and Cortijo, E.: Millennial-scale climatic variability between 340 000 and 270 000 years ago in SW Europe: evidence from a NW Iberian margin pollen sequence, Clim. Past, 5, 53–72, doi:10.5194/cp-5-53-2009, 2009.

Deuser, W. G. and Ross, E. H.: Seasonally Abundant Planktonic-Foraminifera of the Sargasso Sea – Succession, Deep-Water Fluxes, Isotopic Compositions, and Paleoceanographic Implications, J. Foramin. Res., 19, 268–293, 1989.

de Vernal, A. and Hillaire-Marcel, C.: Natural variability of Greenland climate, vegetation, and ice volume during the past million years, Science, 320, 1622–1625, doi:10.1126/science.1153929, 2008.

Dickson, A. J., Leng, M. J., and Maslin, M. A.: Mid-depth South Atlantic Ocean circulation and chemical stratification during MIS-10 to 12: implications for atmospheric CO2, Clim. Past, 4, 333–344, 2008, http://www.clim-past.net/4/333/2008/.

Droxler, A. W., Alley, R. B., Howard, W. R., Poore, R. Z., and Burckle, L. H.: Introduction: unique and Exceptionally Long Interglacial Marine Isotope Stage 11: Window into Earth Warm Future Climate, in: Earth's Climate and Orbital Eccentricity: the Marine Isotope Stage 11 Question, edited by: Droxler, A. W., Poore, R. Z., and Burckle, L. H., Geophysical Monograph, American Geophysical Union, Washington, DC, 1–14, 2003.

EPICA Members: Eight glacial cycles from an Antarctic ice core, Nature, 429, 623–628, 2004.

Fairbanks, R. G., Wiebe, P. H., and Be, A. W. H.: Vertical-

Distribution and Isotopic Composition of Living Planktonic-Foraminifera in the Western North-Atlantic, Science, 207, 61–63, 1980.

Fiúza, A. F. G.: Hidrologia e Dinamica das Aguas Costeiras de Portugal, Faculdade de Ciências da Universidade de Lisboa, Universidade de Lisboa, Lisbon, 294 pp., 1984.

Flores, J.-A., Marino, M., Sierro, F. J., Hodell, D. A., and Charles, C. D.: Calcareous plankton dissolution pattern and coccolithophore assemblages during the last 600 kyr at ODP Site 1089 (Cape Basin, South Atlantic): paleoceanographic implications, Palaeogeography, Palaeoclimatology, Palaeoecology, 196, 409–426, 2003.

Flower, B. P., Oppo, D. W., McManus, J. F., Venz, K. A., Hodell, D. A., and Cullen, J. L.: North Atlantic intermediate to deep water circulation and chemical stratification during the past 1 Myr, Paleoceanography, 15, 388–403, 2000.

Fratantoni, D. M.: North Atlantic surface circulation during the 1990's observed with satellite-tracked drifters, J. Geophys. Res., 106, 22067–22093, 2001.

Ganssen, G.: Dokumentation von küstennahem Auftrieb anhand stabiler Isotope in rezenten Foraminiferen vor Nordwestafrika, Meteor-Forschungsergebnisse, C37, 1–46, 1983.

Guo, Z. T., Biscaye, P., Wei, L. Y., Chen, X. F., Peng, S. Z., and Liu, T. S.: Summer monsoon variations over the last 1.2 Ma from the weathering of loess-soil sequences in China, Geophys. Res. Lett., 27, 1751–1754, 2000.

Hall, I. R. and Becker, J.: Deep Western Boundary Current variability in the subtropical northwest Atlantic Ocean during marine isotope stages 12–10, Geochem. Geophy. Geosy., 8, Q06013, doi:10.1029/2006GC001518, 2007.

Hefter, J.: Analysis of Alkenone Unsaturation Indices with Fast Gas Chromatography/Time-of-Flight Mass Spectrometry, Anal. Chem., 80, 2161–2170, 2008.

Helmke, J. P. and Bauch, H. A.: Comparison of glacial and interglacial conditions between the polar and subpolar North Atlantic region over the last five climatic cycles, Paleoceanography, 18(2), 1036, doi:10.1029/2002PA000794, 2003.

Helmke, J. P., Bauch, H. A., Röhl, U., and Kandiano, E. S.: Uniform climate development between the subtropical and subpolar Northeast Atlantic across marine isotope stage 11, Clim. Past, 4, 181–190, 2008,
http://www.clim-past.net/4/181/2008/.

Hemming, S. R.: Heinrich events: Massive late Pleistocene detritus layers of the North Atlantic and their global climate imprint, Rev. Geophys., 42, 1–43, doi:10.1029/2003RG000128, 2004.

Hodell, D. A., Charles, C. D., and Ninnemann, U. S.: Comparison of interglacial stages in the South Atlantic sector of the southern ocean for the past 450 kyr: implifications for Marine Isotope Stage (MIS) 11, Global Planet. Change, 24, 7–26, doi:10.1016/S0921-8181(99)00069-7, 2000.

Hodell, D. A., Kanfoush, S. L., Venz, K. A., Charles, C. D., and Sierro, F. J.: The Mid-Brunhes Transition in ODP Sites 1089 and 1090 (Subantarctic South Atlantic), in: Earth's Climate and orbital eccentricity: the Marine Isotope Stage 11 Question, edited by: Droxler, A. W., Poore, R. Z., and Burckle, L. H., Geophysical Monograph, American Geophysical Union, Washington, DC, 113–130, 2003.

Hodell, D. A., Channell, J. E. T., Curtis, J. H., Romero, O. E., and Röhl, U.: Onset of "Hudson Strait" Heinrich Events in the Eastern North Atlantic at the end of the Middle Pleistocene Transition (~640 ka)?, Paleoceanography, 23, PA4218, doi:10.1029/2008PA001591, 2008.

Jansen, J. H. F., Kuijpers, A., and Troelstra, S. R.: A Mid-Brunhes Climatic Event: Long-Term Changes in Global Atmosphere and Ocean Circulation, Science, 232, 619–622, 10.1126/science.232.4750.619, 1986.

Ji, J., Ge, Y., Balsam, W., Damuth, J. E., and Chen, J.: Rapid identification of dolomite using a Fourier Transform Infrared Spectrophotometer (FTIR): a fast method for identifying Heinrich events in IODP Site U1308, Mar. Geol., 258, 60–68, 2009.

Jouzel, J., Masson-Delmotte, V., Cattani, O., Dreyfus, G., Falourd, S., Hoffmann, G., Minster, B., Nouet, J., Barnola, J. M., Chappellaz, J., Fischer, H., Gallet, J. C., Johnsen, S., Leuenberger, M., Loulergue, L., Luethi, D., Oerter, H., Parrenin, F., Raisbeck, G., Raynaud, D., Schilt, A., Schwander, J., Selmo, E., Souchez, R., Spahni, R., Stauffer, B., Steffensen, J. P., Stenni, B., Stocker, T. F., Tison, J. L., Werner, M., and Wolff, E. W.: Orbital and Millennial Antarctic Climate Variability over the Past 800 000 Years, Science, 317, 793–796, doi:10.1126/science.1141038, 2007.

Kandiano, E. S. and Bauch, H. A.: Surface ocean temperatures in the north-east Atlantic during the last 500 000 years: evidence from foraminiferal census data, Terra Nova, 15, 265–271, 2003.

Kandiano, E. S. and Bauch, H. A.: Phase relationship and surface water mass change in the Northeast Atlantic during Marine Isotope Stage 11 (MIS 11), Quaternary Res., 68, 445–455, 2007.

Knies, J., Matthiessen, J., Mackensen, A., Stein, R., Vogt, C., Frederichs, T., and Nam, S., II: Effects of Arctic freshwater forcing on thermohaline circulation during the Pleistocene, Geology, 35, 1075–1078, 2007.

Labeyrie, L. D. and Duplessy, J.-C.: Changes in the oceanic $^{13}C/^{12}C$ ratio during the last 140 000 years: high-latitude surface water records., Palaeogeography, Palaeoclimatology, Palaeoecology, 50, 217–240, 1985.

Lambert, F., Delmonte, B., Petit, J. R., Bigler, M., Kaufmann, P. R., Hutterli, M. A., Stocker, T. F., Ruth, U., Steffensen, J. P., and Maggi, V.: Dust-climate couplings over the past 800 000 years from the EPICA Dome C ice core, Nature, 452, 616–619, 2008.

Laskar, J., Robutel, P., Joutel, F., Gastineau, M., Correia, A. C. M., and Levrard, B.: A long-term numerical solution for the insolation quantities of the Earth, Astronomy and Astrophysics, 428, 261–285, doi:210.1051/0004-6361:20041335, 2004.

Lea, D. W., Pak, D. K., and Spero, H. J.: Sea Surface Temperatures in the Western Equatorial Pacific During Marine Isotope Stage 11, in: Earth's Climate and orbital eccentricity: The Marine Isotope Stage 11 Question, edited by: Droxler, A. W., Poore, R. Z., and Burckle, L. H., Geophysical Monograph, American Geophysical Union, Washington, DC, 147–156, 2003.

Levy, M., Lehahn, Y., André, J.-M., Mémery, L., Loisel, H., and Heifetz, E.: Production regimes in the northeast Atlantic: astudy based on Sea-viewing Wide Field-of-view Sensor (SeaWiFS) chlorophyll and ocean general circulation model mixed layer depth, J. Geophys. Res., 110, C07S10, doi:10.1029/2004JC002771, 2005.

Lisiecki, L. E. and Raymo, M.: A Pliocene-Pleistocene stack of 57 globally distributed benthic ^{18}O records, Paleoceanography, 20, PA1003, doi:10.1029/2004PA001071, 2005.

Loulergue, L., Schilt, A., Spahni, R., Masson-Delmotte, V., Blunier, T., Lemieux, B., Barnola, J.-M., Raynaud, D., Stocker, T.

F., and Chappellaz, J.: Orbital and millennial-scale features of atmospheric CH4 over the past 800 000[thinsp]years, Nature, 453, 383–386, 2008.

Loutre, M. F. and Berger, A.: Marine Isotope Stage 11 as an analogue for the present interglacial, Global Planet. Change, 36, 209–217, 2003.

Lüthi, D., Le Floch, M., Bereiter, B., Blunier, T., Barnola, J.-M., Siegenthaler, U., Raynaud, D., Jouzel, J., Fischer, H., Kawamura, K., and Stocker, T. F.: High-resolution carbon dioxide concentration record 650 000–800 000 years before present, Nature, 453, 379–382, 2008.

Martrat, B., Grimalt, J. O., Shackleton, N. J., de Abreu, L., Hutterli, M. A., and Stocker, T. F.: Four Climate Cycles of Recurring Deep and Surface Water Destabilizations on the Iberian Margin, Science, 317, 502–507, doi:10.1126/science.1139994, 2007.

McCartney, M. S. and Talley, L. D.: The Subpolar Mode Water of the North Atlantic Ocean, J. Phys. Oceanogr., 12, 1169–1188, 1982.

McManus, J., Oppo, D. W., and Cullen, J. L.: A 0.5-million-year record of millennial-scale climate variability in the North Atlantic, Science, 283, 971–975, 1999.

McManus, J., Oppo, D., Cullen, J., and Healey, S.: Marine Isotope Stage 11 (MIS 11): analog for Holocene and Future Climate?, in: Earth's Climate and orbital eccentricity: the Marine Isotope Stage 11 Question, edited by: Droxler, A. W., Poore, R. Z., and Burckle, L. H., Geophysical Monograph, American Geophysical Union, Washington, DC, 69–86, 2003.

Müller, P. J., Kirst, G., Ruhland, G., von Storch, I., and Rosell-Melé, A.: Calibration of the alkenone paleotemperature index Uk37' based on core-tops from the eastern South Atlantic and the global ocean (60° N–60° S), Geochim. Cosmochim. Ac., 62, 1757–1772, 1998.

Oppo, D. W., McManus, J., and Cullen, J. C.: Abrupt climate change events 500 000 to 340 000 years ago: Evidence from subpolar North Atlantic sediments, Science, 279, 1335–1338, 1998.

Oppo, D. W., Keigwin, L. D., McManus, J. F., and Cullen, J. L.: Persistent suborbital climate variability in marine isotope stage 5 and Termination II, Paleoceanography, 16, 280–292, 2001.

Ortiz, J. D., Mix, A. C., Rugh, W., Watkins, J. M., and Collier, R. W.: Deep-dwelling planktonic foraminifera of the northeastern Pacific Ocean reveal environmental control of oxygen and carbon isotopic disequilibria, Geochim. Cosmochim. Ac., 60, 4509–4523, 1996.

Ottens, J. J.: Planktic foraminifera as North Atlantic water mass indicators, Oceanol. Acta, 14, 123–140, 1991.

Peliz, A., Dubert, J., Santos, A. M. P., Oliveira, P. B., and Le Cann, B.: Winter upper ocean circulation in the Western Iberian Basin – Fronts, Eddies and Poleward Flows: an overview, Deep Sea Research Part I: Oceanographic Research Papers, 52, 621–646, 2005.

Petit, J. R., Jouzel, J., Raynaud, D., Barkov, N. I., Barnola, J. M., Basile, I., Bender, M., Chapellaz, J., Davis, M., Delaygue, G., Delmotte, M., Kotlyakov, V. M., Legrand, M., Lipenkov, V. Y., Lorius, C., Pépin, L., Ritz, C., Saltzman, E., and Stievenard, M.: Climate and atmospheric history of the past 420 000 years from the Vostok ice core, Antarctica, Nature, 399, 429–436, 1999.

Pflaumann, U., Sarnthein, M., Chapman, M., de Abreu, L., Funnell, B., Huels, M., Kiefer, T., Maslin, M., Schulz, H., Swallow, J., van Kreveld, S. , Vautravers, M., Vogelsang, E., and Weinelt, M.: Glacial North Atlantic: sea-surface conditions reconstructed by GLAMAP 2000 Paleoceanography, 18(3), 1065, doi:10.1029/2002PA000774, 2003.

Pierre, C., Belanger, P., Saliège, J. F., Urrutiaguer, M. J., and Murat, A.: Paleoceanography of the western Mediterranean during the Pleistocene: oxygen and carbon isotope records at Site 975, in: Proceedings ODP, Scientific Results, edited by: Zahn, R., Comas, M. C., and Klaus, A., Ocean Drilling Program, College Station, TX, 481–488, 1999.

Poli, M. S., Thunell, R. C., and Rio, D.: Millennial-scale changes in North Atlantic Deep Water circulation during marine isotope stages 11 and 12: Linkage to Antarctic climate, Geology, 28, 807–810, 2000.

Prokopenko, A. A., Williams, D. F., Kuzmin, M. I., Karabanov, E. B., Khursevich, G. K., and Peck, J. A.: Muted climate variations in continental Siberia during the mid-Pleistocene epoch, Nature, 418, 65–68, 2002.

Raffi, I., Backman, J., Fornaciari, E., Palike, H., Rio, D., Lourens, L., and Hilgen, F.: A review of calcareous nannofossil astrobiochronology encompassing the past 25 million years, Quaternary Sci. Rev., 25, 3113–3137, 2006.

Reverdin, G., Niiler, P. P., and Valdimarsson, H.: North Atlantic Ocean surface currents, J. Geophys. Res., 108(C1), 3002, doi:10.1029/2001JC001020, 2003.

Rickaby, R. E. M. and Elderfield, H.: Evidence from the high-latitude North Atlantic for variations in Antarctic Intermediate water flow during the last deglaciation, Geochem. Geophy. Geosy., 6, Q05001, 1–12, 2005.

Rios, A. F., Perez, F. F., and Fraga, F.: Water Masses in the Upper and Middle North-Atlantic Ocean East of the Azores, Deep-Sea Res. Pt. A, 39, 645–658, 1992.

Rodrigues, T., Voelker, A. H. L., Grimalt, J. O., Abrantes, F., and Naughton, F.: Iberian Margin Sea Surface Temperature during MIS 15 to 9 (580–300 ka): Glacial suborbital variability vs. interglacial stability. Paleoceanography, in review, 2010.

Ruddiman, W. F.: Late Quaternary deposition of ice-rafted sand in the subpolar North Atlantic (lat 40° to 65° N), Geol. Soc. Am. Bull., 88, 1813–1827, 1977.

Ruddiman, W. F.: Orbital changes and climate, Quaternary Sci. Rev., 25, 3092–3112, 2006.

Salgueiro, E., Voelker, A., Abrantes, F., Meggers, H., Pflaumann, U., Loncaric, N., Gonzalez-Alvarez, R., Oliveira, P., Bartels-Jonsdottir, H. B., Moreno, J., and Wefer, G.: Planktonic foraminifera from modern sediments reflect upwelling patterns off Iberia: insights from a regional transfer function, Mar. Micropaleontol., 66, 135–164, doi:10.1016/j.marmicro.2007.09.003, 2008.

Salgueiro, E., Voelker, A. H. L., de Abreu, L., Abrantes, F., Meggers, H., and Wefer, G.: Temperature and productivity changes off the western iberian margin during the last 150 ky, Quaternary Sci. Rev., 29, 680–695, doi:10.1016/j.quascirev.2009.11.013, 2010.

Shackleton, N. J.: The last interglacial in the marine and terrestrial records, P. R. Soc. London, 6, 183–190, 1969.

Shackleton, N. J.: Attainment of isotopic equilibrium between ocean water and the benthonic foraminifera genus Uvigerina: isotopic changes in the ocean during the last Glacial, Colloques Internationaux du C. N. R. S., 219, 203–209, 1974.

Shackleton, N. J., Hall, M. A., and Vincent, E.: Phase relationships

between millennial-scale events 64 000–24 000 years ago, Paleoceanography, 15, 565–569, 2000.

Siegenthaler, U., Stocker, T. F., Monnin, E., Luethi, D., Schwander, J., Stauffer, B., Raynaud, D., Barnola, J.-M., Fischer, H., Masson-Delmotte, V., and Jouzel, J.: Stable Carbon Cycle-Climate Relationship During the Late Pleistocene, Science, 310, 1313–1317, 2005.

Spahni, R., Chappellaz, J., Stocker, T. F., Loulergue, L., Hausammann, G., Kawamura, K., Flückiger, J., Schwander, J., Raynaud, D., Masson-Delmotte, V., and Jouzel, J.: Atmospheric Methane and Nitrous Oxide of the Late Pleistocene from Antarctic Ice Cores, Science, 310, 1317–1321, 2005.

Spero, H. J. and Lea, D. W.: The cause of carbon isotope minimum events on glacial terminations, Science, 296, 522–525, 2002.

Stein, R., Hefter, J., Grützner, J., Voelker, A., and Naafs, B. D. A.: Variability of surface-water characteristics and Heinrich-like Events in the Pleistocene mid-latitude North Atlantic Ocean: Biomarker and XRD records from IODP Site U1313 (MIS 16 – 9), Paleoceanography, 24, PA2203, doi:10.1029/2008PA001639, 2009.

Stirling, C. H., Esat, T. M., Lambeck, K., McCulloch, M. T., Blake, S. G., Lee, D.-C., and Halliday, A. N.: Orbital Forcing of the Marine Isotope Stage 9 Interglacial, Science, 291, 290–293, 2001.

Toucanne, S., Zaragosi, S., Bourillet, J. F., Cremer, M., Eynaud, F., Van Vliet-Lanoe, B., Penaud, A., Fontanier, C., Turon, J. L., Cortijo, E., and Gibbard, P. L.: Timing of massive "Fleuve Manche" discharges over the last 350 kyr: insights into the European ice-sheet oscillations and the European drainage network from MIS 10 to 2, Quaternary Sci. Rev., 28, 1238–1256, 2009.

Tzedakis, P. C., Andrieu, V., de Beaulieu, J. L., Crowhurst, S., Follieri, M., Hooghiemstra, H., Magri, D., Reille, M., Sadori, L., Shackleton, N. J., and Wijmstra, T. A.: Comparison of terrestrial and marine records of changing climate of the last 500 000 years, Earth Planet. Sci. Lett., 150, 171–176, 1997.

Tzedakis, P. C., Roucoux, K. H., de Abreu, L., and Shackleton, N. J.: The Duration of Forest Stages in Southern Europe and Interglacial Climate Variability, Science, 306, 2231–2235, 2004.

Tzedakis, P. C., Hooghiemstra, H., and Palike, H.: The last 1.35 million years at Tenaghi Philippon: revised chronostratigraphy and long-term vegetation trends, Quaternary Sci. Rev., 25, 3416–3430, 2006.

Tzedakis, P. C., Pälike, H., Roucoux, K. H., and de Abreu, L.: Atmospheric methane, southern European vegetation and low-mid latitude links on orbital and millennial timescales, Earth Planet. Sci. Lett., 277, 307–317, 2009.

van Aken, H. M.: The hydrography of the mid-latitude Northeast Atlantic Ocean – Part III: the subducted thermocline water mass, Deep-Sea Res. Pt. I: Oceanographic Research Papers, 48, 237–267, 2001.

Venz, K. A., Hodell, D. A., Stanton, C., and Warnke, D. A.: A 1.0 Myr record of Glacial North Atlantic Intermediate Water variability from ODP site 982 in the northeast Atlantic, Paleoceanography, 14, 42–52, 1999.

Villanueva, J., Grimalt, J. O., Cortijo, E., Vidal, L., and Labeyrie, L.: A biomarker approach to the organic matter deposited in the North Atlantic during the last climatic cycle, Geochim. Cosmochim. Ac., 61, 4633–4646, 1997.

Voelker, A., Martin, P., Lebreiro, S., and Abrantes, F.: Millennial-scale Deep/Intermediate Water Changes at the Mid-depth Portuguese Margin During Marine Isotope Stage (MIS) 11, Quaternary International, 436, 167–168, 2007.

Voelker, A. H. L.: Zur Deutung der Dansgaard-Oeschger Ereignisse in ultra-hochauflösenden Sedimentprofilen aus dem Europäischen Nordmeer., DSc dissertation, Berichte-Reports, Institut für Geowissenschaften, Universität Kiel, no. 9, University of Kiel, Kiel, Germany, 278 pp., 1999.

von Grafenstein, R., Zahn, R., Tiedemann, R., and Murat, A.: Planktonic δ^{18}O records at Sites 976 and 977, Alboran Sea: stratigraphy, forcing, and paleoceanographic implications, in: Proceedings ODP, Scientific Results, edited by: Zahn, R., Comas, M. C., and Klaus, A., Ocean Drilling Program, College Station, TX, 469–479, 1999.

Wang, P., Tian, J., Cheng, X., Liu, C., and Xu, J.: Carbon reservoir changes preceded major ice-sheet expansion at the Mid-Brunhes event, Geology, 31, 239–242, 2003.

Watanabe, O., Jouzel, J., Johnsen, S., Parrenin, F., Shoji, H., and Yoshida, N.: Homogeneous climate variability across East Antarctica over the past three glacial cycles, Nature, 422, 509–512, 2003.

Weirauch, D., Billups, K., and Martin, P.: Evolution of Millennial-Scale Climate Variability During the Mid Pleistocene, Paleoceanography, 23, PA3216, doi:10.1029/2007PA001584, 2008.

Yin, Q. Z. and Berger, A.: Insolation and CO_2 contribution to the interglacial climate before and after the Mid-Brunhes Event, Nature Geosci., 3, 243–246, doi:10.1038/ngeo771, 2010.